Acoustic Tweezers for Particle and Fluid Micromanipulation

Michael Baudoin, Jean-Louis Thomas

Acoustical tweezers for particles and fluids micromanipulation.

M. Baudoin[1], J.-L. Thomas,[2]

[1]Univ. Lille, CNRS, Centrale Lille, ISEN, Univ. Valenciennes, UMR 8520 - IEMN, International laboratory LIA/LICS, F-59000 Lille, France; email: michael.baudoin@univ-lille1.fr; ORCID: 0002-2714-2629
[2]Sorbonne Université, CNRS, Institut des NanoSciences de Paris, INSP - UMR 7588, F-75005 Paris, France; email: jean-louis.thomas@upmc.fr

Annu. Rev. Fluid Mech. 2020. 52:1–30

https://doi.org/10.1146/((please add article doi))

Keywords

Tweezers, acoustical vortices, acoustic radiation pressure, acoustic streaming

Abstract

The contactless collective or selective manipulation of microscopic objects is powerfully enabled by acoustical tweezers. Trapping is achieved without pre-tagging with several order of magnitude larger forces at same input power than optical tweezers, limiting spurious heating and enabling damage-free displacement and orientation of biological samples. In addition, the availability of acoustical coherent sources from kHz to GHz frequencies enables the manipulation of a wide spectrum of particle sizes. After an introduction of the key physical concepts behind fluid and particles manipulation with acoustic radiation pressure and acoustic streaming, we will highlight the emergence of specific wave fields, called acoustical vortices, as a mean to manipulate particles selectively and in 3D. These acoustic vortices can also be used to generate hydrodynamic vortices whose topology is controlled by the topology of the wave. We will conclude this review by a viewpoint on the field future directions.

1. Introduction

Acoustical tweezers enable the collective and selective manipulation of particles and fluids with the use of two nonlinear effects: the acoustic radiation pressure and the acoustic streaming. For particles manipulation, they offer complementary skills compared to their magnetic and optical analogues. Indeed, one of the first recognized issues of optical tweezers is that the tightly focused laser beam heats the sample and may induce photo-damage (Ashkin et al. (1986), Svoboda & Block (1994)). This limits the use of optical tweezers for the manipulation of bio-samples, especially when substantial forces ($\geq$ 100 pN) are required. On the other hand, magnetic tweezers have a low trap stiffness since the field is rather constant at the particle scale and most importantly, magnetic tweezers only enable the manipulation of magnetic particles or require pre-tagging of the target particle (Neuman & Nagy (2008)). All these difficulties are overcome with acoustical tweezers: Indeed, both acoustical and optical radiation pressure are proportional to the intensity of the incoming wave divided by the celerity of the wave. Since acoustic waves speed in liquids is five orders of magnitude smaller than light speed, much larger forces can be applied in acoustics than in optics at same wave intensity, therefore limiting deleterious heating (Baresch, Thomas & Marchiano (2016)). Moreover, acoustical tweezers do not require pre-tagging. Finally, since ultrasonic sources are available from kHz to GHz frequencies, particles of sizes ranging from hundred nanometers to millimeter sizes can be trapped and manipulated with these devices.

These attractive features have led to early development of acoustical traps (King (1934), Sölner & Bondy (1936)). The first systems were based on plane standing waves to trap particles at the nodes or antinodes of the wave depending on their acoustic properties. It is interesting to note that the emergence of miniaturized transducers enabling on-chip particle trapping (Ding et al. (2012), Tran, Marmottant & Thibault (2012)) has led to a renewed interest in the field, with tremendous developments for practical applications in biology (Ozcelik et al. (2018)). On the one hand, plane standing wave fields are interesting when only one particle is present in the system, for the collective manipulation of multiple objects or for particles sorting. On the other hand, the multiplicity of nodes and antinodes precludes any selectivity, i.e. one particle cannot be moved independently of other neighboring particles. Moreover, for 3D particles trapping, the use of standing wave requires to position some transducers (or reflectors) on each side of the trapping area.

The development of *selective tweezers* (with the ability to manipulate particles individually), however requires to strongly localize the acoustic energy in the area of interest. A natural idea is thus to use focalized waves, as in optics (Wu (1991)). Nevertheless, one persisting difficulty that impeded the development of selective acoustical tweezers is that most particles of interest (elastic particles, cells, microorganisms) are denser and stiffer than the fluid and hence are trapped at pressure nodes of acoustic fields (Gorkov (1962)). Thus, they would be expelled from the wave focus. Another difficulty is to obtain a 3D trap with a one-sided tweezers, i.e. with a transducer located on only one side of the manipulated samples (for obvious practical reasons). The difficulty arises since scattering forces resulting from the interaction of the beam with the particle tend naturally to push the particles in the direction of the wave propagation. Trapping of particles in this direction with a limited aperture of the transducer is thus a real challenge.

To solve these issues, it was first proposed by (Baresch, Thomas & Marchiano (2013b)) to use some specific wave fields called focalized acoustical vortices. These focalized helical waves are spinning around a phase singularity, wherein the intensity vanishes, lead-

ing to a minimum of the pressure intensity at the focal point surrounded by a bright ring of high intensity, ensuring the existence of an acoustical trap. These waves possess some fascinating properties: they are non-diffracting and carry orbital momentum (Hefner & Marston (1999)). The ability of such wave fields to trap particles in 3D with a one-sided wave synthesis system has been first demonstrated experimentally by (Baresch, Thomas & Marchiano (2016)). More recently it has been shown by (Riaud et al. (2017a), Baudoin et al. (2019a)) that the relatively complex transducers arrays used by Baresch et al. can be replaced by a single interdigitated transducer, whose spiraling shape encodes the phase of the field like a hologram, hence enabling the selective manipulation of particles in a standard microscopy environment. These spiraling transducers are cheap, flat, easily integrable and compatible with disposable substrates, enabling their widespread use by the scientific community. Another possibility consists in using acoustic lens made of metascreen (Li et al (2015), Jiang et al (2016)) or spiral grating (Jiménez et al (2016)).

It is also interesting to note that acoustical vortices not only enable particles manipulation but also fluid manipulation with the use of acoustic streaming (Anhäuser, Wunenburger & Brasselet (2012), Riaud et al. (2014), Hong, Zhang & Drinkwater (2015)). In particular, they enable the synthesis of hydrodynamic vortices, whose topology is controlled by the topology of the acoustical vortex and not by the boundary conditions. This might lead to tremendous developments in microfluidics or in fundamental study of hydrodynamic vortices.

In section 2, we will introduce the fluids mechanics concepts at the origin of particles and fluids manipulation. Section 3 discusses the classical manipulation of particles with standing wave fields and the numerous application at micro-scales. In section 4, we introduce some specific wave fields, called acoustical vortices and show how they can be used for 3D selective particles and fluids manipulation. Finally, we conclude this review by a viewpoint on the field future directions.

2. Nonlinear acoustics for fluid and particles manipulation

2.1. Nonlinear average equations in acoustics

At first (linear) order, the time averaged net force exerted on a particle and the time average fluid flow induced by an acoustic field are null. Thus the manipulation of particles and fluids requires second order nonlinear effects. One of this effect, called *acoustic radiation pressure*, is a net force applied at the interface between two media with different acoustic properties. This force enables the manipulation of particles but also the deformation of fluid interfaces. A second effect, called *acoustic streaming*, is a flow produced by the attenuation of an acoustic wave and the resulting transfer of pseudo-momentum from the wave to the fluid. Depending on the origin of the wave attenuation, acoustic streaming is generally divided into *bulk acoustic streaming* (also called "Eckart streaming") due to thermoviscous damping of the wave in the bulk of the propagating fluid and *boundary streaming* (also called "Rayleigh streaming"), due to wave attenuation at the boundaries resulting from the existence of a viscous boundary layer.

In this section we will derive a set of coupled constitutive equations, which enable to compute (i) the nonlinear propagation of acoustic waves, (ii) bulk acoustics streaming and (iii) the force applied on a particle (resulting from acoustic radiation pressure and bulk streaming). All these equations will be derived in the limit of low acoustic Mach number,

low acoustic Reynolds number and low hydrodynamic Reynolds number. Since this review is focused on freely propagating waves, boundary streaming will be mostly discarded.

Constitutive equations For the sake of simplicity, we will consider here the case of liquids. Hence, the starting point of the following derivation is the isentropic[1] compressible Navier-Stokes equations, wherein thermal effects are neglected:

$$\text{Mass balance:} \quad \frac{\partial \rho}{\partial t} + \nabla.(\rho \mathbf{v}) = 0 \tag{1}$$

$$\text{Momentum balance:} \quad \frac{\partial \rho \mathbf{v}}{\partial t} + \nabla.(\rho \mathbf{v} \otimes \mathbf{v}) = -\nabla p + \mu \Delta \mathbf{v} + \left(\frac{\mu}{3} + \xi\right) \nabla \nabla.\mathbf{v} \tag{2}$$

$$\text{Entropy balance} \quad ds = 0 \tag{3}$$

$$\text{Equation of state:} \quad p = p(\rho), \text{ with } \left.\frac{\partial p}{\partial \rho}\right|_s = c_o^2 \text{ and } \left.\frac{\partial^2 p}{\partial \rho^2}\right|_s = \Gamma \tag{4}$$

and ρ, p, $\mathbf{v}$ the density, pressure and velocity fields respectively, μ the dynamic viscosity, ξ the bulk viscosity, c_o the sound speed, $\Gamma = \frac{Bc_o^2}{A\rho_o}$, and $A = \rho_o c_o^2$ and B are two classic acoustics coefficients introduced in nonlinear acoustics.

Thermal effects (wave thermal damping and fluid heating) can be neglected in liquids compared to their viscous counterpart (since they are proportional to $\gamma - 1$, with γ the heat capacity ratio, close to 1 in most liquids). The following theory could be nevertheless completed to account for thermal effects.

Field decomposition Following (Riaud et al. (2017b)), we then introduce a relevant decomposition of each field f into (i) a hydrostatic contribution (in absence of acoustic excitation) f_o, periodic fluctuations corresponding to the acoustic wave perturbation $\tilde{f}$ and time averaged contributions $\bar{f}$ [2]:

$$\rho = \rho_o + \tilde{\rho} + \bar{\rho} \tag{5}$$

$$p = p_o + \tilde{p} + \bar{p} \tag{6}$$

$$\mathbf{v} = \tilde{\mathbf{v}} + \bar{\mathbf{v}} \tag{7}$$

Since the fluid is assumed to be at rest in absence of acoustic excitation, $\mathbf{v}_o = \mathbf{0}$. Mathematically, these fields are defined as $\bar{f} =< f - f_o >$ with $<>$ the time averaging operator, $\tilde{f} = f - f_o - \bar{f}$ (implying $< \tilde{f} >= 0$). We also assume $\bar{f} \ll \tilde{f} \ll f_o$.

[1] The fact that viscous effects are considered in the momentum balance but not in the equation of entropy might seem contradictory since viscous effects contribute to the increase of entropy. In fact, since viscous damping is weak and the contribution of viscous effects to the increase of entropy is nonlinear, this approximation is consistent up to second order. See ref (Coulouvrat (1992)) for a demonstration with asymptotic analysis.

[2] This decomposition differs from the classical decomposition into a zero, first and second order field in the sense that acoustic wave perturbation can also contain nonlinear effects as we shall see later.

Averaged equations and bulk acoustic streaming Time averaging of the constitutive equations 1 to 4 up to second order gives:

$$\frac{\partial \bar{\rho}}{\partial t} + \rho_o \nabla.(\bar{\mathbf{v}}) + \frac{1}{c_o^2}\nabla.\bar{\mathbf{I}} = 0 \tag{8}$$

$$\frac{\partial}{\partial t}\left(\rho_o \bar{\mathbf{v}} + \frac{1}{c_o^2}\bar{\mathbf{I}}\right) + \rho_o \nabla.\langle\tilde{\mathbf{v}} \otimes \tilde{\mathbf{v}}\rangle = -\nabla\bar{p} + \mu\Delta\bar{\mathbf{v}} + \left(\frac{\mu}{3} + \xi\right)\nabla\nabla.\bar{\mathbf{v}} \tag{9}$$

$$\bar{p} = c_o^2\bar{\rho} + \frac{\Gamma}{2}\left\langle\tilde{\rho}^2\right\rangle \tag{10}$$

with $\bar{I} = \langle\tilde{p}\tilde{\mathbf{v}}\rangle$ the intensity vector, representing the flux of acoustic energy. These equations are the constitutive equations of the average flow $\bar{\mathbf{v}}$ produced by an acoustic wave, which by definition corresponds to *acoustic streaming*. We can note that, by neglecting the fourth order terms $\nabla.(\bar{\mathbf{v}} \otimes \bar{\mathbf{v}})$, we neglected nonlinear hydrodynamics terms. These equations are therefore limited to slow streaming and cannot describe turbulent flows.

Away from boundaries (and the viscous boundary layer), these equations can be simplified with weakly restrictive hypotheses: In the mass conservation (Equation 8), the divergence of the intensity vector (third term) corresponds to the viscous dissipation of acoustic energy, which remains weak compared to inertial terms in most media at usual frequencies. This is quantified by the so-called acoustic Reynolds number $Re_{ac} = \rho c_o^2/\omega\mu(4/3 + \frac{\xi}{\mu})$ which is also the ratio between the *acoustic attenuation length* $L_a = \rho c_o^3/\omega^2\mu(4/3 + \frac{\xi}{\mu})$ (the characteristic distance of the wave damping) and the wavelength λ. As a consequence, the condition $Re_{ac} \ll 1$ ensures that the wave is not attenuated over a distance comparable to the wavelength. The reverse situation only happens in very viscous fluids or at frequencies higher than GHz in water. If we assume $Re_{ac} \ll 1$ and consider only the steady average flow (after the transient state), we obtain the classical Stokes equation:

$$\nabla\bar{\mathbf{v}} = 0 \tag{11}$$

$$\mu\Delta\bar{\mathbf{v}} - \nabla\bar{p} + \mathcal{F} = \mathbf{0} \tag{12}$$

with a forcing term (Nyborg (1953)):

$$\mathcal{F} = -\rho_o \nabla.\langle\tilde{\mathbf{v}} \otimes \tilde{\mathbf{v}})\rangle \tag{13}$$

corresponding to the source of acoustic streaming. As expected, this source is a nonlinear average effect resulting from the acoustic field $\tilde{\mathbf{v}}$. Owing to its simplicity, this expression of the streaming source term has been widely used to compute acoustic steady streaming numerically. Nevertheless, as we shall see, this expression should be avoided as it contains some terms that do not contribute to bulk acoustic streaming but instead to acoustic radiation pressure and can lead to large numerical errors in simulations.

Periodic fluctuations: nonlinear propagation of the wave The equations of the periodic fluctuations up to second order can be simply obtained by subtracting average equations (1 to 4) to the constitutive Equations (8 to 10):

$$\frac{\partial \tilde{\rho}}{\partial t} + \rho_o \nabla . \tilde{\mathbf{v}} = -\nabla . \ll \tilde{\rho}\tilde{\mathbf{v}} \gg \tag{14}$$

$$\rho_o \frac{\partial \tilde{\mathbf{v}}}{\partial t} + \nabla \tilde{p} - \mu \Delta \tilde{\mathbf{v}} - \mu b \nabla \nabla . \tilde{\mathbf{v}} = \frac{\partial}{\partial t} \ll \tilde{\rho}\tilde{\mathbf{v}} \gg -\rho_o \nabla . \ll \tilde{\mathbf{v}} \otimes \tilde{\mathbf{v}} \gg \tag{15}$$

$$\tilde{p} - c_o^2 \tilde{\rho} = \frac{\Gamma}{2} \ll \tilde{\rho}^2 \gg \tag{16}$$

with $b = 1/3 + \xi/\mu$ and the operator $\ll\gg$ is defined by $\ll \tilde{f}\tilde{g} \gg = \tilde{f}\tilde{g} - < \tilde{f}\tilde{g} >$. The left hand sides of these equations corresponds to the linear equations of damped acoustic waves. The right hand sides of these equations represent nonlinear effects affecting the propagation of the acoustic waves. Following (Riaud et al. (2017b)), these equations can be combined to obtain the celebrated Kuznetsov equation (Kuznetsov (1970)) describing the nonlinear propagation of acoustic waves:

$$\frac{\partial^2 \tilde{\phi}}{\partial t^2} - c_o^2 \Delta \tilde{\phi} - \frac{\mu b}{\rho_o} \frac{\partial}{\partial t} \Delta \tilde{\phi} = \frac{\partial}{\partial t} \left(\frac{B}{2Ac_o^2} \ll \left(\frac{\partial \tilde{\phi}}{\partial t} \right)^2 \gg + \ll \left(\nabla \tilde{\phi} \right)^2 \gg \right) \tag{17}$$

with $\tilde{\phi}$ the velocity potential ($\tilde{\mathbf{v}} = \nabla \tilde{\phi}$). In this equation, the first two terms on the lhs simply correspond to d'Alembert wave equation, the third term on the lhs accounts for the wave viscous damping, while the terms on the rhs corresponds to nonlinear effects affecting the wave propagation. Here we assumed that $\tilde{\mathbf{v}} = \nabla \tilde{\phi}$ and thus that the fluctuation field is irrotational. This is correct away from viscous boundary layers, since acoustic modes are by definition irrotational.

It can be noticed that the contribution of the nonlinear terms to the wave propagation can be sized by comparing the characteristic length of the wave propagation L_c to the so-called *shock distance* $L_s = c_o^2/\omega\beta U_{ac}$, where U_{ac} is the magnitude of the acoustic velocity perturbation and $\beta = 1 + B/2A$ the so-called nonlinear parameter. Indeed, nonlinear effects are small but nevertheless cumulative. Thus, they can play a significant role over this characteristic distance. The main effect is the generation of harmonics and the transfer of energy to these harmonics, which can eventually turn a sinusoidal wave into an acoustical shock wave (at the origin of the name "Shock distance"). In many practical applications, the nonlinear propagation terms can be neglected.

Simplification of the bulk streaming source term Following (Lighthill (1978)) and (Riaud et al. (2017b)), the streaming source term $\mathcal{F} = -\rho_o \nabla . \langle \tilde{\mathbf{v}} \otimes \tilde{\mathbf{v}} \rangle$ can be recast into a gradient term that does not contribute to acoustic streaming but only to the acoustic radiation force and another term that is the sole source of bulk streaming:

$$\mathcal{F} = -\nabla \bar{\mathcal{L}} + \frac{\omega^2 \mu b}{\rho_o c^4} \bar{\mathbf{I}} \tag{18}$$

with $\bar{\mathcal{L}} = \bar{\mathcal{K}} - \bar{\mathcal{V}}$ the average acoustic Lagrangian, $\bar{\mathcal{K}} = 1/2\rho_o < \tilde{\mathbf{v}}^2 >$ the average acoustic kinetic energy and $\bar{\mathcal{V}}$ the average potential energy $\bar{\mathcal{V}} = \langle \tilde{p}^2 \rangle / (2\rho_o c_o^2)$. The main assumption to obtain this equation is that the fluctuation field $\tilde{\mathbf{v}}$ is irrotational. Then, if we introduce the dynamic pressure of the streaming flow $\bar{p}^s = \bar{p} + \bar{\mathcal{L}} = c_o^2 \bar{\rho} + \Gamma/2 \left\langle \tilde{\rho}^2 \right\rangle + \bar{\mathcal{L}}$, then the Stokes equation of the streaming flow (Equation 12) can be rewritten under the form:

$$\mu \Delta \bar{\mathbf{v}} - \nabla \bar{p}^s + \mathcal{F}^{\mathcal{S}} = 0 \text{ with } \mathcal{F}^{\mathcal{S}} = \frac{\omega^2 \mu b}{\rho_o c^4} \bar{\mathbf{I}} \tag{19}$$

$\mathcal{F}^{\mathcal{S}}$ being the sole source of acoustic streaming. This equation shows that the gradient term plays no role on acoustic streaming. It also shows, as expected, that the streaming source depends on the wave damping ($\propto \omega^2 \mu b$) and the average acoustic intensity $\bar{\mathbf{I}}$.

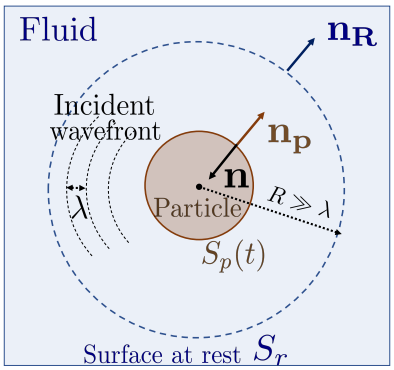

Figure 1: Geometry and notations used of the calculation of the force exerted on a particle by an incident acoustic wave.

Force applied on a particle and acoustic radiation force Now that we have obtained equations for acoustic streaming, we can derive the average force applied on a particle. This force $\bar{\mathbf{F}}_p$ is simply the time average of the stress exerted on the moving interface $S_p(t)$ of the particle:

$$\bar{\mathbf{F}}_p = \left\langle \iint_{S_p(t)} \sigma.\mathbf{n_p} dS \right\rangle \tag{20}$$

with $\sigma = -p\mathbf{1} + 2\mu\mathbf{D} + (\xi - 2\mu/3)(\nabla.\mathbf{v})\mathbf{1}$ the stress tensor and $\mathbf{n_p}$ the vector normal to the surface of the particle pointing outward with respect to the particle, **Figure 1**. The difficulty to perform this integral comes from the vibration of the particle surface induced by the acoustic wave, and thus the fact that it is not fixed. To overcome this difficulty, we can start by introducing flux of momentum tensor $\mathcal{B} = \rho\mathbf{v} \otimes \mathbf{v} - \sigma$, and rewrite the momentum balance under the form:

$$\frac{\partial \rho \mathbf{v}}{\partial t} + \nabla.\mathcal{B} = \mathbf{0}. \tag{21}$$

Then, we can introduce a closed surface at rest surrounding the particle S_r, and integrate this momentum equation over a volume $V(t)$ bounded on one side by the vibrating surface $S_p(t)$ and the other side by the fixed surface S_r (see **Figure 1**). The divergence theorem gives:

$$\iiint_{V(t)} \frac{\partial \rho \mathbf{v}}{\partial t} dV + \iint_{S_p(t)} \mathcal{B}.\mathbf{n} dS + \iint_{S_r} \mathcal{B}.\mathbf{n_R} dS = \mathbf{0} \tag{22}$$

with $\mathbf{n} = -\mathbf{n_p}$ and $\mathbf{n_R}$ the normal to the surface at rest S_r pointing outward with respect to $V(t)$. Then using, the Reynolds transport theorem:

$$\frac{\partial}{\partial t} \iiint_{V(t)} \rho \mathbf{v} dV = \iiint_{V(t)} \frac{\partial \rho \mathbf{v}}{\partial t} dV + \iint_{S_p(t)} \rho \mathbf{v}\mathbf{v}.\mathbf{n} dS, \tag{23}$$

the time average of Equation 22 becomes:

$$\bar{\mathbf{F}}_p = \left\langle \iint_{S_p(t)} \sigma.\mathbf{n} dS \right\rangle = -\iint_{S_R} \bar{\mathcal{B}}.\mathbf{n_R} dS \tag{24}$$

with the average momentum flux tensor equal to $\bar{\mathcal{B}} = \rho_o \langle \tilde{\mathbf{v}} \otimes \tilde{\mathbf{v}} \rangle + (p_o + \bar{p})\mathbf{1} - 2\mu\bar{\mathbf{D}} - (\xi - 2\mu/3)\nabla.\bar{\mathbf{v}}$ up to second order. Finally considering $\bar{p} = \bar{p}^s - \bar{\mathcal{L}}$ and $\nabla.\bar{\mathbf{v}} = 0$, we obtain the following final expression of the force applied on a particle [3]:

$$\bar{\mathbf{F}}_p = \bar{\mathbf{F}}_{rad} + \bar{\mathbf{F}}_{str} \tag{25}$$

$$\text{with } \bar{\mathbf{F}}_{rad} = \iint_{S_R} (-\rho_o \tilde{\mathbf{v}} \otimes \tilde{\mathbf{v}} + \bar{\mathcal{L}}).\mathbf{n_R} dS \tag{26}$$

$$\text{and } \bar{\mathbf{F}}_{str} = \iint_{S_R} (-\bar{p}^s \mathbf{1} + 2\mu\bar{\mathbf{D}}).\mathbf{n_R} dS \tag{27}$$

As we will see in the next section, the first component of the force $\bar{\mathbf{F}}_{rad}$ is the so-called *radiation force* applied on the particle, while obviously the second component of the force is simply the force applied on the particle by the average flow, i.e. bulk acoustic streaming.

Nonlinear acoustics in a nutshell As a conclusion to this section, acoustic wave propagation, bulk acoustic streaming and the force applied on a particle can be summarized by the following set of coupled nonlinear equations:

$$\text{Acoustic wave propagation (linear case): } \frac{\partial^2 \tilde{\phi}}{\partial t^2} - c_o^2 \Delta\tilde{\phi} - \frac{\mu b}{\rho_o}\frac{\partial}{\partial t}\Delta\tilde{\phi} = 0 \tag{28}$$

$$\text{Acoustic streaming: } \mu\Delta\bar{\mathbf{v}} - \nabla\bar{p}^s + \mathcal{F}^{\mathcal{S}} = 0, \text{ with: } \mathcal{F}^{\mathcal{S}} = \frac{\omega^2 \mu b}{\rho_o c^4}\bar{\mathbf{I}} \text{ and } \bar{\mathbf{I}} = <\tilde{p}\tilde{\mathbf{v}}> \tag{29}$$

$$\text{Force exerted on a particle: } \bar{\mathbf{F}}_p = \bar{\mathbf{F}}_{rad} + \bar{\mathbf{F}}_{str} \tag{30}$$

$$\text{with the radiation stress: } \bar{\mathbf{F}}_{rad} = \iint_{S_R} (-\rho_o \tilde{\mathbf{v}} \otimes \tilde{\mathbf{v}} + \bar{\mathcal{L}}).\mathbf{n_R} dS \tag{31}$$

$$\text{and the streaming force: } \bar{\mathbf{F}}_{str} = \iint_{S_R} (-\bar{p}^s \mathbf{1} + 2\mu\bar{\mathbf{D}}).\mathbf{n_R} dS \tag{32}$$

2.2. Radiation pressure: an historical perspective

2.2.1. Origin of the term radiation pressure. The force $\mathbf{F_p}$, applied by a wave on a particle is at first order an oscillating phenomena whose temporal average is zero. The existence of a non-zero average force $\bar{\mathbf{F}}_\mathbf{p}$ dates back to Kepler's observation of the orientation of comets tail with respect to the light emitted by the sun. The corpuscular theories of light at that time are probably at the origin of the term "*radiation pressure*" to name the mean force per unit area, $\bar{\mathcal{P}}_{em}$, in reference to the pressure in a gas. In this analogy, the radiation pressure of a light wave is always directed perpendicular to the surface of the enlightened object.

[3] Since integration is performed here on a closed surface, Equations 26 and 27 are unaffected by any constant C, i.e. $\bar{p} = \bar{p}^{s\prime} - \bar{\mathcal{L}}'$ with $\bar{\mathcal{L}}' = \bar{\mathcal{L}} + C$ and $\bar{p}^{s\prime} = \bar{p}^s + C$ would lead to the same force applied on the particle. This constant is nevertheless important when Rayleigh radiation pressure is under consideration, see section 2.2.2 for the definition of *Rayleigh radiation pressure* and *Langevin radiation pressure*, and the discussion in section 2.2.4.

Maxwell was the first to propose a coherent theory of this phenomenon and demonstrated that light can exert a force in its direction of propagation instead (Jackson (1962)). In this theory, the radiation pressure is given by the average of the electromagnetic stress tensor. A more correct denomination would therefore be the radiation stress and this point is at the origin of many misunderstandings on this subject. This nonlinear phenomenon proportional to the square of the electromagnetic field has (for a plane wave propagating along the z-axis) an amplitude equal to the energy density of the wave, $\bar{\mathcal{P}}_{em} \cdot \mathbf{z} = \bar{E}_{em}$. By analogy with point mechanics, the existence of a nonzero mean force leads to the existence of a linear momentum carried by electromagnetic waves. This hypothesis will be confirmed by relativity and will lead to the equivalence between mass and energy that will relate photon momentum and energy.

2.2.2. Radiation pressure in acoustics. It was in this context, just before the advent of relativity, that Rayleigh proposed and modeled the existence of a radiation pressure for acoustic waves in fluids. He studied the plane wave case and initially obtained an expression identical to optics: the radiation pressure is a second order phenomena equal to the time-averaged acoustic energy density $\bar{E}_a$ (Rayleigh (1902)):

$$\bar{\mathcal{P}}_a = \bar{E}_a = \bar{\mathcal{K}} + \bar{\mathcal{V}} \tag{33}$$

This naturally led him to postulate the existence of a linear momentum carried by an acoustic wave and to explain the acoustic radiation pressure by an exchange of momentum similarly to optics, following the point of view of Poynting (McIntyre (1981), Post (1960)). Nevertheless, an acoustic wave propagates in a material medium and taking into account the non-linearity of its state equation, Rayleigh obtained a second expression (Rayleigh (1905), Post (1953)):

$$\bar{\mathcal{P}}_a = \beta \bar{E}_a \tag{34}$$

where $\beta = 1 + B/(2A)$. This differentiates the acoustic case from the optical one, the material medium must be taken into account and nowadays this expression is referred to as the *Rayleigh radiation pressure*. The proportionality of acoustic radiation pressure and energy density was demonstrated by (Altberg (1903)). The situation studied by Rayleigh corresponds to a plane wave of infinite lateral extension or a plane mode in a wave-guide. This situation is quite far from the practical case where one seeks to manipulate solid or fluid particles completely immersed in a fluid. The first to propose a relevant model for this case was Langevin in a colloquium. His work was nevertheless only published nine years later by (Biquard (1932a)). Using Kelvin circulation theorem, he showed that in the stationary regime, the mean pressure difference between two points O and M of a fluid is equal to the difference of acoustic energy density in these two points, $\bar{p}^L_O - \bar{p}^L_M = \bar{E}_O - \bar{E}_M$, here the superscript, L, stands for Lagrangian coordinates to differentiate from Eulerian coordinates. Selecting for M a point where the medium is at rest, yields:

$$\bar{p}^L = \bar{E}_a + C \tag{35}$$

with C a constant. As a consequence, the component related to the non-linearity of the state equation, see Equation 34, contributes only through a uniform pressure, C, which consequently cannot give rise to any overall force for a completely immersed object since it is applied on all side on the object. Thus, he recovered Equation 33, the equivalent to the

optical case known today as *Langevin radiation pressure*. The computation in Eulerian coordinates was also made assuming an irrotationnal particle velocity and using the unsteady Bernouilli theorem, this was published in a second article (Biquard (1932b)):

$$\bar{p} = p^L - 2\bar{K} = -\bar{\mathcal{L}} + C \tag{36}$$

These two calculations of the average pressure in a fluid in Lagrangian and Eulerian coordinates (Equations 35 and 36), are called *first and second Langevin relations*. This last relation has been revisited by (King (1934), Richter (1940), Bopp (1940)) among others. We propose here a new version. Indeed, Equation 19 yields $\nabla \bar{p}^s = 0$ for an ideal fluid, so that Equation 36 is recovered from the definition $\bar{p}^s = \bar{p} + \bar{\mathcal{L}}$.

At this stage, some confusions remained on the origin and nature of acoustic radiation pressure: First, the average force per unit area exerted by the acoustic wave was considered at that time as a pressure, i.e a stress tensor that is equal to the identity tensor times a scalar. Second, the linear momentum carried by an acoustic wave and its transfer to another medium was considered by Rayleigh as responsible for the radiation pressure.

2.2.3. Radiation stress tensor and acoustic momentum. This situation was reanalyzed by Brillouin (Brillouin 1925a, Brillouin (1925b)). A good account in English of the content of his papers, published originally in French, can be found in his book (Brillouin (1938)).

First, he challenges the existence of a momentum carried by a longitudinal acoustic wave in a fluid, i.e he demonstrates that acoustic waves can very well exist without any average momentum [4].

Indeed, the mean momentum in both Eulerian and Lagrangian coordinates is:

$$\rho_0 \bar{\mathbf{v}}^L = \langle \rho \mathbf{v}^E \rangle = \langle \tilde{\rho}\tilde{\mathbf{v}} \rangle + \rho_0 \bar{\mathbf{v}} \tag{37}$$

Hence a zero average momentum, i.e a zero material velocity $\bar{\mathbf{v}}^L = 0$ does not prevent the existence of an acoustic wave (field $\tilde{\rho}$, $\tilde{\mathbf{v}}$) but instead leads to a non-zero average velocity in Eulerian coordinates $\bar{\mathbf{v}} = -\langle \tilde{\rho}\tilde{\mathbf{v}} \rangle / \rho_0$. This second order difference between the particle velocity in Lagrangian and Eulerian coordinates $\langle \tilde{\rho}\tilde{\mathbf{v}} \rangle / \rho_0 = \bar{\mathbf{v}}^L - \bar{\mathbf{v}}$ is called the *Stokes drift*. Hence the acoustic radiation pressure exerted by these waves cannot be explained by an exchange of momentum. The quantity $\langle \tilde{\rho}\tilde{\mathbf{v}} \rangle$ is not a true momentum and should be called instead pseudo-momentum or quasi-momentum for quasi-particles like phonons (Peierls (1985), McIntyre (1981), Thomas, Marchiano & Baresch (2017)).

Second, he stated that the force exerted on the object is the integral of the Cauchy stress on its surface oriented toward the outside, see Equation 20. In the special case of a perfect fluid, the Cauchy stress tensor is the opposite of the pressure times the unit tensor, $-p\mathbf{1}$. The radiation force is thus the average of this quantity:

$$\bar{\mathbf{F}}_p = -\langle \iint_{S_p(t)} p \mathbf{n_p} dS \rangle = -\langle \iiint_{V(t)} \nabla p dV \rangle \tag{38}$$

where we use the divergence theorem to get the second equality. It is important to note that in this expression, the surface of the object $S_p(t)$ driven by the acoustic wave deforms to follow the vibrations of the surrounding medium and thus ensure the continuity of the

[4] i.e. without any mass flow since acoustic waves are supported by a medium and the average momentum also correspond to the average mass flow.

normal velocity at the interface. Since the surface elements varies in time, the average and integral operators do not commute and $\tilde{p}$ will contribute to the radiation pressure. This definition of the radiation force is difficult to use in practice. An exception is Bjerknes force on a small spherical bubble. At the bubble scale, the pressure gradient is assumed uniform and integration leads to $\bar{\mathbf{F}}_p = -\langle V(t)\nabla\tilde{p}\rangle$, where $V(t)$ is the bubble volume (Bjerknes (1906)). This case illustrates that radiation pressure is a nonlinear phenomenon: the pressure at first order is null on average but cannot be neglected since the surface is varying in time. Third, Brillouin substituted Lagrangian coordinates for Eulerian coordinates in this surface integral. On the one hand this approach enables to recover a surface at rest to perform the integral and on the other hand, the Cauchy stress tensor is transformed into the first Piola-Kirchoff stress tensor. Since the surface is now fixed, the temporal average operation commutes with the integration and thus integrating the first Piola-Kirchoff average on the rest surface yields the radiation pressure. The first Piola-Kirchoff stress tensor is the momentum flux in the momentum conservation equation in Lagrangian coordinates. The averaged flux of momentum can be finite even if the averaged momentum is null. While this definition is convenient for radiation pressure in solids, an expression in Euler coordinates is preferable in fluids. So Brillouin proposed to use the averaged flux of momentum in Eulerian coordinates on a fixed surface surrounding the object. He noted that that going from moving surface elements to fixed ones is exactly compensated by subtracting the averaged Reynolds stress tensor, so that:

$$\bar{\mathbf{F}}_p = -\langle \iint_{S_p(t)} p\mathbf{n_p} dS\rangle = -\langle \iint_{S_R} (p\mathbf{1} + \rho \mathbf{v}\otimes\mathbf{v}).\mathbf{n_R} dS\rangle = -\iint_{S_R} \bar{\mathcal{B}}\mathbf{n_R} dS \tag{39}$$

with S_R a fixed surface surrounding the object, **Figure 1**, and:

$$\bar{\mathcal{B}} = (\bar{p} + p_0)\mathbf{1} + \rho_0\langle\tilde{\mathbf{v}}\otimes\tilde{\mathbf{v}}\rangle \tag{40}$$

for an inviscid flow. The tensorial nature of radiation pressure has been experimentally verified by (Hertz & Mende (1939), Herrey (1955)). This derivation has been generalized by (Beissner (1998)) in a fluid and the average fluxes of momentum in Eulerian and Lagrangian coordinates differ only by a curl that does not contribute to the force on a completely immersed object. The direct derivation of Equation 39 from Equation 38, originally introduced by (Hasegawa et al. (2000)), uses the Reynolds transport theorem and has been presented with more generality in section 2.1.

2.2.4. Integral expression of the force exerted on an immersed particle. To get an expression valid at second order, one may use the expression of the mean pressure Equation 36 and substitute it in Equation 40:

$$\bar{\mathcal{B}} = -\bar{\mathcal{L}}\mathbf{1} + (p_0 + C)\mathbf{1} + \rho_0\langle\tilde{\mathbf{v}}\otimes\tilde{\mathbf{v}}\rangle \tag{41}$$

When the object is completely immersed in a perfect fluid (corresponding to *Langevin radiation pressure*), the integration over a fixed surface surrounding the object cancels the uniform part of the isotropic terms $(p_0+C)\mathbf{1}$ and hence the radiation force is obtained by the average of the following tensor (Brillouin (1936), Bopp (1940), Richter (1940), Post (1953), Borgnis (1953)), Equation 31:

$$\bar{\mathcal{B}} = -\bar{\mathcal{L}}\mathbf{1} + \rho_0\langle\tilde{\mathbf{v}}\otimes\tilde{\mathbf{v}}\rangle \tag{42}$$

Note that this tensor is completely determined by the average of quadratic expression involving $\tilde{p}$ and $\tilde{\mathbf{v}}$ and hence, the radiation force on a completely immersed object does not depend on the medium nonlinearity that is contained in the constant C. Thus we recover the optical case features. This holds as long as the pressure like term has time to relax and give at equilibrium a uniform pressure throughout the fluid.

However, when the wave is of infinite aperture or confined in a waveguide, (corresponding to *Rayleigh radiation pressure*), this isotropic uniform term plays a role. Thus the constant C must be determined from the boundary conditions (Brillouin 1925a). For a plane progressing wave oriented along x-axis impinging on an absorbing target whose average position is fixed, all fields have an uniform amplitude. So we can deduce from mass conservation that $\bar{\rho} = 0$ since the whole volume is fixed in average . From Equation 10, we get $\bar{p} = B/A\bar{\mathcal{V}}$. Since for a plane progressive wave $\bar{\mathcal{V}} = \bar{\mathcal{K}} = 1/2\bar{E}_a$, $\bar{p} = B/(2A)\bar{E}_a$ and $\rho_0\langle\tilde{v}_i\tilde{v}_j\rangle = 1/2\bar{E}_a\delta_{11}$. So the radiation stress tensor, Equation 40, reduces to $(p_0 + B/(2A)\bar{E}_a)\delta_{ij} + 1/2\bar{E}_a\delta_{11}$. The lateral pressure is $p_0 + B/(2A)\bar{E}_a$ while on the axis of propagation, we get $p_0 + \beta\bar{E}_a$. If the outside pressure is p_0 the excess pressure from the inside is $\beta\bar{E}_a$, i.e. the *Rayleigh radiation pressure*, Equation 34.

2.3. Axial radiation force on a sphere

As underlined above (Equation 42), the radiation pressure tensor depends only on the acoustic field at first order. However, these fields are the sum of the incident and scattered field and thus it is necessary to compute this latter before performing the integration on a surface at rest arbitrary located around the object. These two steps have been achieved by (King (1934)) for a rigid sphere using Equation 36. (Embleton (1954)) extended these results to the radiation pressure on a rigid sphere set at the focus of a spherical incident wave. (Yosioka & Kawasima (1955)) solved the problem of a compressible fluid sphere and then (Hasegawa & Yosioka (1969)) the one of an elastic sphere but in a plane incident wave only using Equation 42. Later, the work of Embleton was generalized to take into account the elasticity of the sphere (Chen & Apfel (1996)). An essential step is the computation of the scattered waves and hence the scattering coefficient. For an incident longitudinal plane wave and an elastic sphere, the first derivation was made by (Faran (1951)). In all these works extending, axisymmetry is used to simplify considerably the task (Hasegawa, Ochi & Matsuzawa (1981)). Mathematically, the displacement vector in the elastic spherical particle can be decomposed into a scalar and a vector potential using Helmholtz' decomposition. For an incident longitudinal plane wave propagating along the z-axis, the axial symmetry enables do introduce only one component for the vector potential in spherical coordinates: $\mathbf{A} = (0, 0, A(r, \theta))$. The complete problem is thus reduced to two scalars, both solutions of Helmholtz's equation. The two potentials are then written as an infinite sum of spherical modes without azimuthal dependence. The boundary conditions at the sphere surface provide the relation between incident and scattered waves for each spherical mode. This is important to note that only the force component in the beam direction can be calculated with this approach. These two limitations (axial symmetry and force component in the beam direction) forbade using these models for tweezers investigations and led only to experimental confirmation of theory (Klein (1938), Rudnick (1977), Hasegawa (1977)), local acoustic fields measurements complementary of radiation force balance (Rooney (1973)) and levitation traps (Sölner & Bondy (1936)).

2.4. Bulk acoustic streaming: an historical perspective

As the story of acoustic radiation pressure, the history of acoustic streaming also starts with the work of Rayleigh (Rayleigh (1884)). Aroused by the observations of (Faraday (1831)) and (Dvorak (1874)) of the flows produced by vibrating plates and Kund's tubes respectively, Rayleigh developed the first theory of the flow induced by an acoustic wave damped by its interactions with the walls of a tube. In this first type of acoustic streaming, the flow results from the wave damping induced by shear stresses in the viscous boundary layer, where the fluid velocity decays to match the velocity of the boundary. This type of streaming is now referred to as *boundary streaming or Rayleigh streaming*. Later on, with the advent of piezoelectric generators, many scientist have reported strong flows of air or liquid in the direction of the acoustic wave propagation referred at this time as "quartz wind". It was first demonstrated by (Eckart (1948)) (for liquids) that, in this case, the flow results from the viscous attenuation of the wave in the bulk of the fluid [5]. This second type of acoustic streaming is now referred to as *bulk streaming or Eckart streaming*. Eckart obtained his results (i) by developing compressible isentropic Navier-Stokes equations into zero, first (linear) and second (nonlinear) orders contributions, (ii) by combining the mass and momentum equations at second order and (iii) by separating the second terms contributing to the nonlinear propagation of the wave from the one contributing to the steady flow by taking the divergence and curl of this combined equations, respectively. In this way, he obtained an unsteady diffusion equation for the vorticity (curl of the velocity) at second order, corresponding to acoustic streaming:

$$\frac{\partial \mathbf{\Omega_2}}{\partial t} - \frac{\mu}{\rho_o}\Delta \mathbf{\Omega_2} = \frac{b\mu_o}{\rho_o^3}\nabla\rho_1 \times \nabla\frac{\partial \rho_1}{\partial t}, \text{ with } \mathbf{\Omega} = \nabla \times \mathbf{v}_2 \tag{43}$$

He then applied this equations to the flow produced in an infinite tube by a weakly attenuated wave of finite aperture propagating along the axis of the tube without lateral interaction with the walls. His theory was verified soon after by (Libermann (1949)), who nevertheless noticed some differences at large Reynolds number [6]. On the one hand, the advantage of Eckart's formulation is that it does not rely on time averaging and thus these equations enable to describe unsteady bulk streaming. On the other hand, these equations describe the evolution of the vorticity field and (i) it is sometimes difficult to express the boundary conditions in terms of vorticity and (ii) the derivation of the velocity field from the vorticity field requires to solve another set of differential equations. Nyborg proposed a formulation corresponding to a Stokes equation with a source term at the origin of the acoustic streaming (corresponding to Equations 11 to 13). While mathematically sound, his formulation of the source term is to proscribe numerically since it contains some potential terms (see Equations 18), that do not contribute to acoustic streaming, but can be several orders of magnitude larger than the actual source term [7]. Thus small numerical errors on the gradient terms can lead to "numerical acoustic streaming" resulting from numerical dis-

[5] For liquids the viscous damping is dominant. In gases, both thermal and viscous damping contribute to the streaming

[6] Indeed, all these theories based on asymptotic development into different orders contributions are only valid for slow streaming flow (low hydrodynamic Reynolds numbers associated with the steady flow)

[7] See e.g. (Shiokawa (1990)), who compared the two terms in the study of acoustic streaming produced by surface acoustic waves and erroneously neglected the term that actually contributes to acoustic streaming)

sipation. (Lighthill (1978)) identified this gradient term and later on (Riaud et al. (2017b)) isolated the sole source of bulk acoustic streaming and expressed it as a function of the intensity vector (see Equation 19). These authors also demonstrated that the bulk streaming source term can be spatially filtered as the small structures of the acoustic field do not contribute to acoustic streaming. In 1953, (Westervelt, P.J. (1953)) extended Eckart's work and reconciliated bulk and boundary streaming in a single formulation. He showed that his formulation enables to recover these two types of streaming as limit cases.

Since these pioneering work on bulk streaming, many effects have been studied such as transient streaming (Rudenko (1971)), the influence of diffraction by the edges of the beam (Kamakura (1996), Moudjed et al. (2014)), the effect of the nonlinear propagation of the wave (Romanenko (1960), Stanikov (1967)), weakly nonlinear flows at intermediate Reynolds numbers in the limit of the conservation of the flow symmetry (Gusev & Rudenko (1979)) or more recently the effect of the fluid inhomogeneity (Karlsen & Bruus (2016)). However, despite these efforts, a proper theory of fast acoustic bulk streaming at high Reynolds numbers is still lacking. We can note that in this short historical review, we did not cover the extensive fields of the flow produced by the interaction of a sound wave with a particle or a bubble, neither we treated the steady streaming produced by incompressible alternative flows (Riley (2001)).

3. Acoustical traps and collective manipulation with standing waves

3.1. Historical development of the field

While the first theoretical works on radiation pressure were performed in optics, the first effective set-up for particles trapping were developed in acoustics. The main reason is the availability of powerful coherent source that will appear later in optics with the development of lasers. Thus collective manipulation of particles with standing waves as a long history going back to Chladni figures and Kundt tubes. Chladni figures illustrates that very small particles are driven mostly by acoustic streaming while the radiation force dominates for larger particles (Hagsäter et al. (2007)). The relation between these standing waves acoustical traps and radiation pressure as modeled by (King (1934)) was clearly established just after (Sölner & Bondy (1936)). (Allen & Rudnick (1947)) observed levitation of different items in standing and progressive waves in air using a very powerful siren operating at 25 kHz. They noted that while relatively large objects could be levitated in standing wave, the trap was unstable for progressive waves. Levitation of bubbles in liquid columns vibrating at low frequency were also observed and explained with Bjerknes force (Bucchanan, Jameson & Oedjoe (1962), Baird (1963)). Piezoelectric sources working at higher frequencies were used thereafter to excite the resonant mode of a cylindrical cavity and levitate a single bubble on the pressure anti-node at low frequencies (Eller (1968), Gould (1968)). Thereafter, these levitation traps were used for studying surface tension and phase transition of liquid drops (Apfel (1981)). Levitation traps were developed both in liquid or in air. In air, the radiation force in acoustics is strong enough to levitate millimeters beads of iridium, the material with the highest density (Xie & Wei (2002)). The observation of agglomeration of red blood cells was related to acoustic standing wave fields and it was initially used to assess potential detrimental hazard in medical imaging (Baker (1972)). When many particles are involved and interact, there are several forces at play and the discrimination can be be rather complex (Coakley et al. (1989)). Nevertheless, it was recognized that radiation pressure in

standing waves could be used for both harvesting and manipulation of small particles (Schram (1984), Whitworth, Grundy & Coakley (1991)) using modulation of either phase or amplitude of the two counterpropagating plane waves.

3.2. Radiation force on drops and elastic spheres in the long Wavelength regime

The most common expression of the radiation force induced by standing waves relies on the assumptions of (i) spherical particles and (ii) excitation in the long wavelength regime (i.e. when the wavelength is much larger than the size of the particle). For bubbles, the force is described by Bjerknes formula. On the contrary, when the contrast of compressibility and density are not too high, e.g elastic particles or drop in a liquid (Gorkov (1962)) developed a model that is used today in most of acoustic traps.

Since the sphere radius is very small compared to the wavelength, $k_0 a << 1$, the monopole and dipole scattering dominate and (Gorkov (1962)) obtained from a multipole expansion a simple expression :

$$\bar{\mathbf{F}}_p = -\nabla \left(\alpha_m \bar{\mathcal{V}} - \alpha_d \bar{\mathcal{K}} \right) \tag{44}$$

$$\text{with } \alpha_m = \frac{4}{3}\pi a^3 \left(1 - \frac{K_0}{K_p} \right) \text{ and } \alpha_d = 4\pi a^3 \left(\frac{\rho_p - \rho_0}{2\rho_p + \rho_0} \right). \tag{45}$$

In this formula, $K_0 = \rho_0 c_0^2$ and $K = \rho_p(4/3c_t^2 - c_l^2)$ are the bulk elasticity of the fluid and solid, ρ_o and ρ_p the fluid and particle densities and a the radius of the particle. The particle longitudinal and transverse wave speeds are noted c_l and c_t respectively. Here the potential and kinetic energy, $\bar{\mathcal{V}}$ and $\bar{\mathcal{K}}$, are computed with the amplitude of the linear incident field at the sphere location. In this expression, the radiation pressure is a potential force that depends on the incident linear fields and the acoustic contrast factor in compressibility and density. This approximation based on a Taylor expansion is valid as long as the kinetic and potential energies are not uniform in any direction. Since it relies on the gradient of the field, it is generally called the *gradient force*. This is the case encountered in standing waves. On the contrary, this force cancels out for a plane progressive wave and the Taylor development must be carried out at next order. This case was also studied by (Gorkov (1962)) and this force is not a gradient force and generally referred to as the *scattering force*. It must be noted that in real fluid, viscosity corrections can be important (Settnes & Bruus (2012)). Thermal dissipation was also considered (Karlsen & Bruus (2015)).

3.3. Particles micro-manipulation with radiation force

Today, a very active field of research combines acoustic standing waves with microfluidics. A lot of promising biological applications are developed in order to separate, concentrate and manipulate particles and in particular biological cells in a label-free environment and with high throughput. The corresponding literature is quite extensive and outside the scope of this review. We redirect an interested reader to existing reviews on the subject (Lenshof & Laurell (2010), Ding et al. (2013), Yeo & Friend (2014), Ozcelik et al. (2018)). Individual particles manipulations are limited by two adverse effects that forbid selectivity. First, standing waves generates traps locations at each nodes or anti-nodes depending on the acoustic contrasts of density and compressibility (see Equation 44), hence preventing the trapping of one particle independently of other neighboring particles. Second, the size and stiffness of the trap is determined by the wavelength and these setup are designed in the long wavelength regime.

4. Selective acoustical tweezers and stirrers

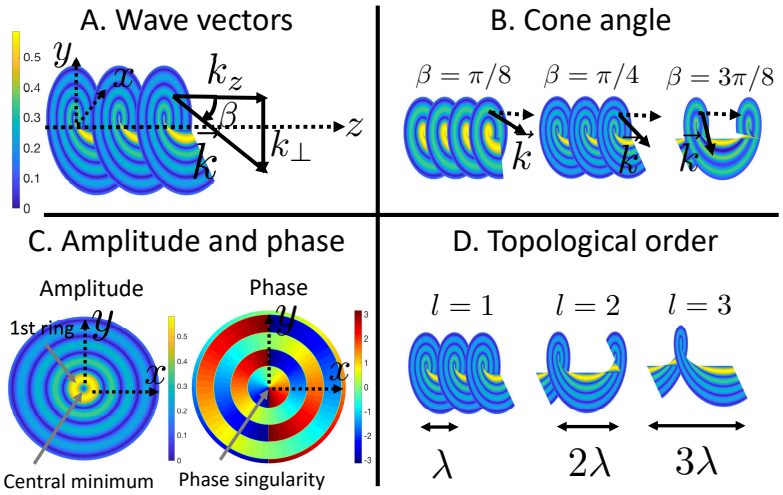

Figure 2: Bessel cylindrical vortices. A. Equiphase surface of a Bessel cylindrical vortex (topological order $l = 1$ and cone angle $\beta = \pi/4$). The colorfield corresponds to the pressure amplitude. The axial component $\mathbf{k_z}$, the lateral component $\mathbf{k}_\perp$ and the total wave vector $\mathbf{k} = \mathbf{k_z} + \mathbf{k}_\perp$ are represented on the graph. Note that $\mathbf{k}_\perp$ is turning around the wave axis as the wave propagates along z-axis. B. Equiphase surfaces of a cylindrical vortex (of topological order $l = 1$) for different cone angles $\beta = \arctan k_\perp/k_z$. As the cone angle increases, the vortex lateral evolution is more rapid while its axial evolution is slower. C. Lateral evolution of the amplitude and phase.The amplitude vanishes on the axis and this central minimum is surrounded by a ring of high intensity. Then the field is a succession of bright and dark rings of decreasing intensities. Inside the first ring, the phase evolves from 0 to 2π when θ goes from 0 to 2π, with a phase singularity at the center. Laterally the phase undergoes some phase jump of π each time the sign of the Bessel function $j_l(kr)$ changes. D. Equiphase surfaces of Bessel cylindrical vortices of different topological orders $l = 1$, $l = 2$ and $l = 3$.

4.1. Spatial localization of the acoustic energy and acoustical vortices

The selective manipulation of a particle, i.e. its manipulation independently of other neighboring particles can only be achieved through spatial localization of the trap and hence the acoustic energy at the scale of the particle. A natural idea to achieve such localization is to use laterally or radially focalized waves (for 2D and 3D selective trapping respectively). This solution adopted in optics is also valid in acoustics for particles attracted at the pressure anti-nodes of an acoustic standing wave field, such as particle less dense and more compressible than the surrounding liquid (see Equations (44) and (**??**)). Nevertheless, particles more stiff and more dense than the surrounding liquid, such as solid particles, cells and most droplets migrate (Gorkov (1962)) toward the pressure nodes of a standing wave field. Such particles would be expelled from the focus of a focalized wave, which precludes their use for many particles of interest. For such particles, it is necessary to concentrate

the energy but with a minimum at the wave focus surrounded by a ring of high intensity, which will ensure particles trapping.

4.1.1. Cylindrical vortices. For 2D particles trapping, this apparently paradoxical problem can be solved by using some specific wave fields called *cylindrical acoustical vortices*, some helical waves spinning around a phase singularity axis (**Figure 2**). These wave structure are called acoustical vortices (similarly to optics where they are referred to as optical vortices) owing to their helical wave front, whose structure resembles a hydrodynamic vortex. Nevertheless, since they are solutions of the wave equation, they do no carry any vorticity. They are sometimes also referred as helical waves. This class of waves were originally introduced by (Nye & Berry (1974)) when he studied wave phase singularities and in particular so-called screw dislocations. This phase singularity ensures a canceling of the amplitude at the beam focus, surrounded by a bright ring which can be used to trap particles laterally (Courtney (2014)). In the field of acoustics, acoustical vortices were first introduced (and experimentally synthesized) by (Hefner & Marston (1999)). Mathematically, these waves structures can be simply introduced as a set of separated variable solutions $\Psi(r,\theta,z) = f(r)g(\theta)h(z)$ of the wave equation in cylindrical coordinates (r,θ,z) in the Fourier space, that is to say Helmholtz equation:

$$\Delta\Psi - k^2\Psi = 0 \Longleftrightarrow \frac{1}{r}\frac{\partial}{\partial r}\left(r\frac{\partial\Psi}{\partial r}\right) + \frac{1}{r^2}\frac{\partial^2\Psi}{\partial\theta^2} + \frac{\partial^2\Psi}{\partial z^2} + k^2\Psi = 0.$$

Indeed, an orthogonal set of solutions of this equation (see SI for the details of the calculation), that we will refer as *Bessel cylindrical vortices* are:

$$\Psi(r,\theta,z,t) = A\,J_l(k_\perp r)\,\exp(i(l\theta + k_z z - \omega t)), \tag{46}$$

with A the amplitude of the vortex, J_l the Bessel function of the first kind of order l, $\boldsymbol{k}$ the wave vector, $k = \|\boldsymbol{k}\| = \omega/c_o^2$ the wave number, c_o the sound speed, $l \in \mathbb{Z}$ an integer called the topological charge, $k_z = \boldsymbol{k}.\boldsymbol{z}$ the projection of the wave vector over the propagation axis $\boldsymbol{z}$ and $k_\perp = k^2 - k_z^2$ (see **Figure 2** for a visual representation of the different parameters). These beams are defined by three parameters: their angular frequency ω, their topological order l and the so-called cone angle $\beta = \arccos(k_z/k)$ which defines the angle between the wave vector $\boldsymbol{k}$ and the propagation axis $\boldsymbol{z}$. We can note, that for $l = 0$, the field becomes invariant over θ and the lateral evolution is given by $J_0(kr)$, which exhibits a maximum in $r = 0$. Thus this wave field is not a vortex but simply a laterally focalized wave. Thus vortices only refer to beams of topological order larger than $|l| > 1$. These waves are propagative over θ and z and stationary over r, with a lateral evolution given by the Bessel function. Bessel functions of order $|l| > 1$ all exhibit a minimum in $r = 0$ and then oscillate inside a decreasing envelope, evolving as $1/\sqrt{r}$.

These waves have good properties for particles lateral trapping. Indeed, the canceling of the Bessel functions $j_l(k_\perp r)$ of order $|l| > 1$ in $r = 0$ and then its increase up to a maximum creates a gradient trap that will maintain the particle at the center.

Some asymptotic forms of these Bessel beams exist in the approximation of small conical angles $\beta \ll 1$ between the wave number and the propagation axis, that is to say in the so-called paraxial approximation. The solutions of the paraxial approximation of Helmholtz equation are the so-called *Laguerre-Gaussian* beams, which take the form:

$$\Psi(r,\theta,z,t) = \frac{A}{w(z)}\left[\frac{\sqrt{2}r}{w(z)}\right]^{|l|} L_p^{|l|}\left(\frac{2r^2}{w(z)^2}\right)\exp\left(\frac{-r^2}{w^2(z)} + i\left(l\theta + (2p+|l|+1)\arctan\left(\frac{z}{z_R}\right) - \frac{r^2 kz}{2(z^2+z_R^2)}\right)\right)$$

with $L_p^{|l|}$ the associated Laguerre polynomial, $w(z) = w_o\sqrt{1+z^2/z_R^2}$ the beam width at position z along the wave propagation axis, w_o the beam waist, $z_R = \pi w_o^2/\lambda$ the Rayleigh range, λ the wavelength, and $(2p+l+1)\arctan(z/z_R)$ the Gouy phase. These waves, are common in optics, since Gaussian beams are good approximation of the field produced by a laser. Their intensity is mostly localized close to the beam axis since their amplitude decreases exponentially as $exp(-r^2/w^2(z))$ with a radial extent equal to $w(z)$. Thus, these waves do not carry an infinite energy and can be synthesized experimentally.

Finally, if we push further the approximation of Bessel beams to vanishing conical angles $\beta \to 0$, then $k_z \to k$ and $k_\perp \to 0$, and Bessel cylindrical vortices turn into so-called *R-vortices*:

$$\Psi = A\, r^l\, e^{i(l\theta + kz - \omega t)}.$$

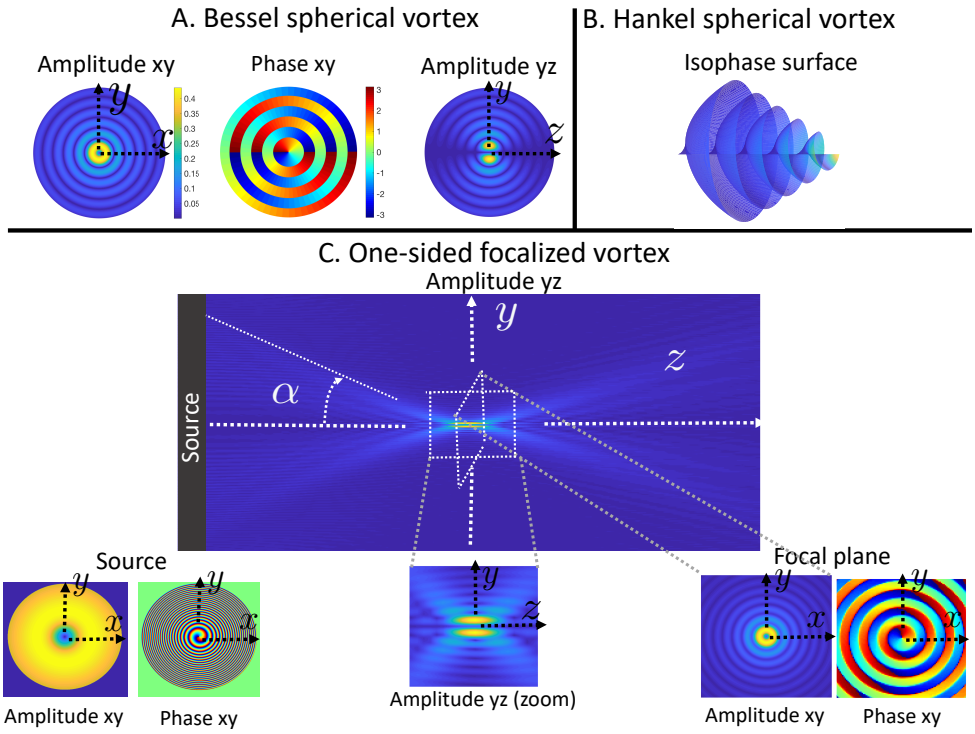

Figure 3: focalized vortices of topological order $(l, m) = (1, 1)$. A. Amplitude and phase of a Bessel spherical vortex, corresponding to Equation 47. B. Isophase surface of a converging Hankel vortex. C. Amplitude and phase of a one-sided focalized vortex. The amplitude in the (y, z) plane shows the focalization of the vortex, pictures on the left hand side show the amplitude and phase in the source plane (x, y), while pictures on the right hand side show the amplitude and phase in the focal plane. α corresponds to the aperture of the source.

4.1.2. Focalized vortices. As first proposed by (Baresch, Thomas & Marchiano (2013b)), an idea to obtain a 3D localized trap is to use the spherical analogues of Bessel cylindrical acoustical vortices, the so-called *Bessel spherical vortices* (**Figure 3.A**). Indeed, these wavefields focalize the energy in 3D, while maintaining a minimum at the focal point.

These fields, as their cylindrical counterparts, are a set of orthogonal separate variables solutions of Helmholtz equation, but this time in spherical coordinates (r, θ, φ):

$$\Psi(r, \theta, \varphi) = A j_l(kr) P_l^m(\cos(\theta)) \exp\left(i(m\varphi - \omega t)\right) \tag{47}$$

with $j_l(kr)$ the spherical Bessel function of the first kind of order $l \in \mathbb{Z}$, P_l^m the associated Legendre polynomial of order $(l,\ m)$, with m the topological charge, an integer verifying $-l \leq m \leq l$. Similarly to cylindrical vortices, we can note that if the topological charge $m = 0$, the field is invariant over φ and thus the wavefield is no more a vortex but simply a focalized wave. In particular, the case $(m, l) = (0, 0)$ corresponds to a spherically focalized wave. Thus we will refer to spherical vortices for waves with topological orders $|m| \geq 1$. These waves are stationary in r and θ and propagative over φ. The central phase singularity is surrounded by a spherical bright shell, which provides a good framework for 3D trapping (see **Figure 3 A, left**). We can nevertheless note that the z-axis remains a specific axis around which the phase is turning (see **Figure 3 A**, center). This specificity can also be seen in Equation 47, since the angle θ refers to the angle with respect to z axis. Owing to the phase singularity over this axis, the amplitude cancels all along this axis (see **Figure 3 A, right**), leading to a weaker trap in this direction.

Spherical vortices carry a finite amount of energy, but their synthesis would require to position some transducers all around a closed surface surrounding the vortex center. Since this is not feasible in most practical situations, an idea is to synthesize a wave which is as close as possible to a spherical vortex, but with a finite aperture. We will will refer in the following to such wavefields as *one-sided focalized vortices* (see **Figure 3.C**). To synthesize these waves a first important element is that similarly to plane standing wave $A\cos(kx)\exp(-i\omega t))$, which can be decomposed into the combination of of two counter-propagating progressive waves $A/2\exp(ikx - \omega t) + A/2\exp(-ikx - \omega t)$, a Bessel spherical vortex is the combination of two Hankel diverging and converging spherical vortices:

$$A j_l(kr) P_l^m(\cos(\theta)) \exp\left(i(m\varphi - \omega t)\right) = \frac{A}{2}\left[h_l^{(1)}(kr) + h_l^{(2)}(kr)\right] P_l^m(\cos(\theta)) \exp\left(i(m\varphi - \omega t)\right)$$

with $h_l^{(1)}$ the Hankel function of the first kind corresponding to the converging part and $h_l^{(2)}$ the Hankel function of the second kind corresponding to the diverging part.

Thus a one-sided focalized vortex can be generated by synthesizing a section of a Hankel converging vortex (Baudoin et al. (2019a)) (see **Figure 3.B** for a representation of the isophase surface of a Hankel vortex). This is possible with a system controlling the phase and/or the amplitude of a vibration on a given surface (which can be for example a portion of sphere or of a plane). An example of a one-sided focalized vortices synthesized from a control disk (wherein the amplitude and phase of the intersection of a Hankel spherical vortex with this disk is imposed) is given on **Figure 3.C**. In this example, the aperture angle is 60^o and the distance between the source and the focal plane is 20λ. This example shows that the interference between the converging Hankel vortex and the diverging Hankel vortex initiated at the passage through the focal point produces a standing gradient trap in the z direction (see **Figure 3.C**, yz zoom). Nevertheless, since the signal is generated from only one side, the propagative part of the wave along z axis tends to push the particle away from the center in the direction of the wave propagation. This is this competition between the axial pushing force and the gradient restoring force, which makes the 3D trapping of particles particularly challenging. In addition the acoustic streaming can also contribute to push the particle away from the trap. In the field of acoustics, Baresch and co-workers

were the first to demonstrate theoretically (Baresch, Thomas & Marchiano (2013b)) and experimentally (Baresch, Thomas & Marchiano (2016)) the ability of these beams to trap particles in the Mie Regime. It is also interesting to note that in the Long Wavelength Regime, Marzo and co-workers have shown (Marzo et al. (2015)) through an optimization algorithm, that acoustical vortices are some optimal wavefields for 3D particle trapping for a given array of transducers with phase control. They also demonstrated that two other types of wavefields, namely *bottle traps* and *twin traps* are optimal for trapping in the direction of propagation and in one lateral direction respectively.

4.2. Selective particles manipulation

In section 2.3, we saw that the scattering coefficients were computed assuming axial symmetry of the problem. For a spherical particle, this assumption restricts the model to incident plane wave or spheres located at the focus of spherical incident beam. It should be noted that either a transversely polarized plane wave or acoustical vortices break the axial symmetry. Scattering of a plane electromagnetic waves by a dielectric sphere has a known solution: the Lorenz-Mie theory. The Debye potentials are here particularly well suited for spherical particles. This case has also been studied for acoustics waves propagating in solids (Einspruch, Witterholt & Truell (1960), Gaunard & Überall (1978)) but the incident wave is always a plane wave, a case irrelevant for tweezers. To go further, there are two main methods developed in optics. The first is to decompose the incident wave into plane waves and then use the previous results for each plane wave modes. The second called generalized Lorenz-Mie theory (GLMT) consists in looking for a decomposition of the arbitrary incident wave in series of modes of the wave equation, generally the spherical basis (Maheu, Gouesbet & Gréhan (1987), Barton, Alexander & Schaub (1988)). This approach led to the first analytic results for radiation pressure exerted by an arbitrary beam on a dielectric sphere (Ren, Gréhan & Gouesbet (1994), Barton, Alexander & Schaub (1989)).

In acoustics, the growing interest in the manipulation of contactless particles has motivated research in this direction. The first strategy was first used and the case of a particle located along the axis of propagation of an incident acoustic beam was modeled. These examples include axisymmetric beams (Marston (2006)) or the more complex wave fronts of a helical Bessel beam (Marston (2008), Marston (2009)). The case of arbitrary incident beam was addressed later (Sapozhnikov & Bailey (2013)) and led to a complete expression of the radiation force.

The second strategy has also been adapted to acoustics and requires three steps. First, a separated variable solution of Helmholtz equation in free space and in spherical coordinates is well known :

$$\phi(\mathbf{r},\omega) = \phi_a \sum_{n=0}^{\infty} \sum_{|m|<n} A_l^m P_l^m(\cos(\theta)) \exp(\imath m\varphi) j_l(k_0 r) \tag{48}$$

The series coefficients A_l^m are called the beam shape coefficients. ϕ_a is an optional factor used to have dimensionless beam shape coefficients. All the previous theory (King (1934), Hasegawa et al. (2000)) assumed azimuthal symmetry and hence $m = 0$. Using normalized spherical harmonics, defined by $Y_l^m = \sqrt{(2l+1)(l-m)!/(4\pi(l+m)!)} P_l^m(\cos(\theta)) \exp(\imath m\varphi)$ leads to another equivalent set of beam shape coefficients $\hat{A}_l^m$. Assuming linear scattering and a spherical basis centered on the spherical scatterer, the beam shape coefficients of the scattered wave are proportional to the incident ones, $R_l^m A_l^m$. However, the boundary

conditions, i.e spherical divergence of the scattered wave, lead to replace Bessel functions by Hankel functions. As in (Hasegawa et al. (2000)), the integration of Equation 42 can then be performed on a fixed spherical surface located in the far field. This generalization was achieved at the same time by (Silva (2011), Baresch, Thomas & Marchiano (2013a)), (Baresch, Thomas & Marchiano (2013a)) was submitted at the time of publication of (Silva (2011)). At this stage, A_l^m and R_l^m are two sets of unknown coefficients and identifying them are the two last steps required to compute the radiation force. The beam shape coefficients are defined by a scalar product between the field and the spherical harmonics. However, they are functions of the position of the sphere and hence their numerical evaluation in a 3D domain is time consuming and requires high precision. To alleviate this problem, different strategies exist (Gouesbet, Lock & Gréhan (2010)). An effective solution used in optics, is to translate and rotate the spherical basis using the additional theorem to follow the sphere and obtain the new coefficients. This solution was adapted to acoustics by (Baresch, Thomas & Marchiano (2013a)). Last, to complete the generalization of (Hasegawa & Yosioka (1969)) to arbitrary incident beams the scattering coefficients, R_l^m, must be computed. This last step was also achieved by (Baresch, Thomas & Marchiano (2013a)). The axisymetry and the resulting simplification made before is no longer valid, see section 2.3. The acoustic displacement field in the elastic particle can be decomposed into three scalar potentials, one for the longitudinal waves, ϕ, and two, the Debye potentials for shear waves ψ, χ, with $\mathbf{A}(r,\theta,\varphi) = \nabla\wedge\nabla\wedge(\mathbf{r}\psi)+\nabla\wedge(\mathbf{r}\chi)$. These potentials are solutions of the Helmholtz scalar equation and thus can be written as series of spherical functions as above. Compared to incident plane wave, the boundary conditions lead to a system of four linear equations relating the four potentials, one in the fluid and three in the elastic particle. This system is actually made of one idependent equation describing one of the shear elastic mode. Therefore, this mode can not be excited by an incident longitudinal wave. The remaining system of three equations is identical with the one obtained by (Faran (1951)). As a consequence, the azimuthal dependence can be dropped : $R_l^m = R_l$. The complete model of (Baresch, Thomas & Marchiano (2013a)) leads to the first numerical study of the radiation pressure exerted by an arbitrary field on an elastic spherical particle. It used the A_l^m and to ease the comparison with (Sapozhnikov & Bailey (2013), Silva (2011)), the radiation force expression are rewritten here with the $\hat{A}_l^m$ set :

$$F_x = -\frac{\langle\tilde{V}\rangle_a}{k_0^2}\sum_{n=0}^{\infty}\sum_{|m|<n} \Im\left(Q_n^{-m}\hat{A}_l^{m*}\hat{A}_{l+1}^{m-1}C_n + Q_n^m\hat{A}_l^m\hat{A}_{l+1}^{m+1*}C_n^*\right) \quad (49)$$

$$F_y = +\frac{\langle\tilde{V}\rangle_a}{k_0^2}\sum_{n=0}^{\infty}\sum_{|m|<n} \Re\left(Q_n^{-m}\hat{A}_l^{m*}\hat{A}_{l+1}^{m-1}C_n + Q_n^m\hat{A}_l^m\hat{A}_{l+1}^{m+1*}C_n^*\right) \quad (50)$$

$$F_z = -2\frac{\langle\tilde{V}\rangle_a}{k_0^2}\sum_{n=0}^{\infty}\sum_{|m|<n} \Im\left(P_n^m\hat{A}_l^{m*}\hat{A}_{l+1}^{m}C_n\right) \quad (51)$$

$\langle\tilde{V}\rangle_a = k_0^2\rho_0|\phi_a|^2/4 = |\phi_a|^2/(4\rho_0c_0^2)$ is a dimensional factor. It should be replaced by $1/(4\rho_0c_0^2)$ if ϕ_a is not introduced in the spherical decomposition of the incident field (Equation 48). $Q_n^m = \sqrt{(n+m+1)(n+m+2)}/\sqrt{(2n+1)(2n+3)}$ and $P_n^m = \sqrt{(n+m+1)(n-m+1)}/\sqrt{(2n+1)(2n+3)}$ are two coefficients related to the amplitude of the spherical harmonics. These two set of coefficients are identical in (Baresch, Thomas & Marchiano (2013a), Sapozhnikov & Bailey (2013)). The ones obtained by (Silva (2011)) contain an error coming from the first step described above that required a reindexing of the series. $C_n = R_n^* + R_{n+1} + 2R_n^*R_{n+1}$ is the coefficient that

explicit the dependence of the radiation force on the scattered waves, $R_n^* R_{n+1}$, or the cross product between incident and scattered waves, $R_n^* + R_{n+1}$. This coefficient can also be written with the S-matrix, $S_n = 1 + 2R_n$, so that $2C_n = S_n^* S_{n+1} - 1$. This relates the outgoing modes of order n and $n+1$, (Sapozhnikov & Bailey (2013), Marston & Zhang (2017)). Using Eq. 32,34 of (Sapozhnikov & Bailey (2013)) it is straightforward to show that the two expressions of the radiation force are identical.

This complete model give quantitative prediction of the radiation force. Some examples are given below for a bead of silica.

One specific feature of selective tweezers compared to standing wave traps is the selectivity. The radial selectivity of a one sided spherical vortex at 50 MHz, a wavelength of 30 μm is shown on **Figure 4 left**. A negative force means that the bead is pulled toward the vortex axis. The trap has a radius of 0.42 λ when the numerical aperture is 0.87, i.e a half angle of 60^o. The radiation pressure scales in nanoNewton, an amplitude relevant for forces at play in biological cells for a weak acoustic pressure of 1 MPa on a bead of silica of radius 0.15 λ. The azimuthal force is of similar amplitude (**Figure 4 right**). A bead initially located in the potential well will spiral around the vortex axis and in the end reach its equilibrium position at $\rho = 0$.

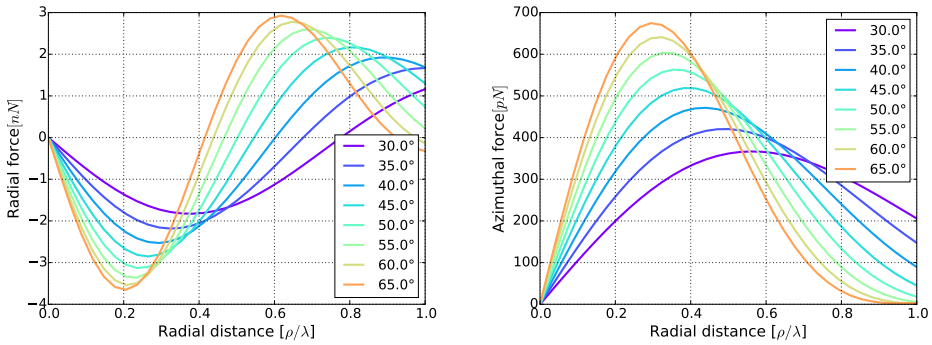

Figure 4: Radial and azimuthal forces of a one sided spherical vortex on a sphere of silica, the wavelength is 30 μm. Forces are computed for a maximum pressure of 1 MPa at focus and a sphere of radius 0.15λ. The trap stiffness and the selectivity increase with the numerical aperture, the half angle is varied from 30^o to 65^o

The axial selectivity and trap stiffness is also strongly dependent on the numerical aperture (**Figure 5 left**). The stiffness, selectivity and force amplitude are weaker in the axial direction compared to the lateral one since the beam is progressive on this axis. The force is positive, (thus pushing the particle), when the bead is located before focus. On the contrary, when the bead is downstream, the axial force is negative and hence pulling the bead toward the focus. This essential and specific feature of optical tweezers (Ashkin (2011)) ensures trapping in the three dimensions. When the radius of the bead is increased, **Figure 5 right** the scattering force increases and for a too large bead the axial trapping is lost.

Three dimensional trapping at the focus of a one-sided focalized acoustical vortex was demonstrated numerically from these formula (Baresch, Thomas & Marchiano (2013b)) and then experimentally (Baresch (2014), Baresch, Thomas & Marchiano (2016)). Here the tweezers pulling restoring force was high enough to compensate the particle weight and the

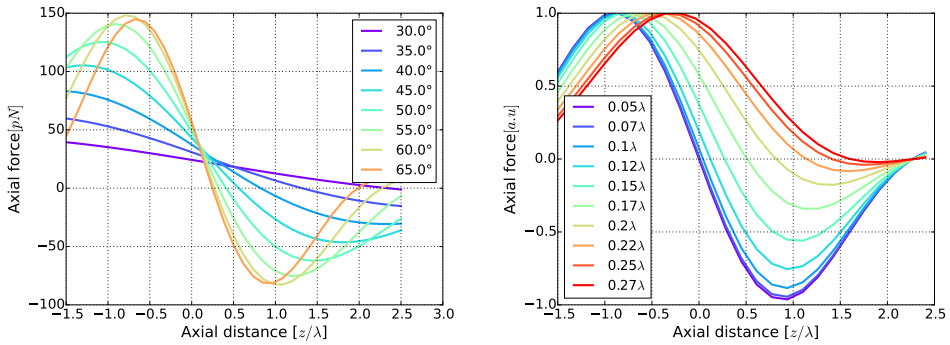

Figure 5: Axial force of a one sided spherical vortex on a sphere of silica, the wavelength is 30 μm. a) The trap stiffness increases with the numerical aperture, the half angle is varied from 30 to 65. The force is computed for a maximum pressure of 1 MPa at focus and a sphere of radius 0.15λ. b) The axial restoring force is lost for too large spheres. The radius of the sphere varies from 0.05 up to 0.27 wavelength.

streaming drag force. A one sided focused acoustical vortex was also able to push upward and then levitate particles in air (Marzo et al. (2015)).

4.3. Fluid manipulation with acoustical vortices

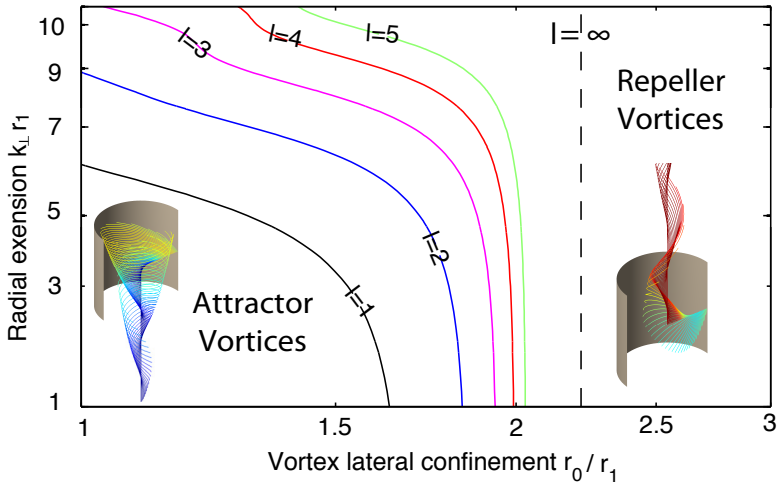

Figure 6: Flow structures induced by Bessel cylindrical vortices. The lines delimit the transition between *attractor vortices* with a poloidal flow oriented toward the center of the source (located downward) and *repeller vortices* corresponding to the classic configuration, wherein the fluid is pushed away from the source. The ratio r_0/r_1 is the ratio between the radius of the cylinder and the lateral extension of the beam. Figure adapted from (Riaud et al. (2014)).

Acoustical vortices carry pseudo-angular momentum. Thus, the nonlinear transfer of this pseudo-angular momentum to the fluid through the wave attenuation results in a streaming flow whose topology is mainly controlled by the topology of the acoustic vortex. The first estimation and observation of this effect was provided by (Anhäuser, Wunenburger & Brasselet (2012)). Then, (Riaud et al. (2014)) resolved the complete problem by extending Eckart's theory to the case of Bessel cylindrical acoustical vortices. Starting from Eckart's vorticity diffusion equation:

$$\Delta\bar{\boldsymbol{\Omega}} = -\frac{b}{\rho_o^2}\nabla\tilde{\rho}\times\nabla\frac{\partial\tilde{\rho}}{\partial t},$$

with $\bar{\boldsymbol{\Omega}} = \nabla\times\bar{\mathbf{v}}$ and $\tilde{\rho}$ given by Equation 46, they were able to compute the velocity field in the same configuration as Eckart, i.e. in an infinitely long cylinder of radius r_0 axially enlightened by a beam of finite aperture $r_1 < r_0$. They demonstrated that the acoustical streaming in this configuration is the superposition of a poloidal flow also observed by Eckart in the case of a plane wave and a toroidal flow that relies on the helical nature of the acoustical vortex. Interestingly, they showed that in some specific configurations, the direction of the poloidal flow can be reversed compared to the plane wave case, and the fluid can recirculate toward the center of the transducer (**Figure 6**). This can be explained by the existence of a shadow zone at the center of the beam wherein the fluid can recirculate.

Soon after, the toroidal flow predicted by this theory was shown experimentally by (Hong, Zhang & Drinkwater (2015)) in an essentially 2D configuration. More recently, (Baresch, Thomas & Marchiano (2018)) evidenced the flow produced by a one-sided focalized vortex and demonstrated that the fluid is both pushed in the direction of the wave propagation and set in rotation around the propagation axis due to the helical nature of the wave. From a theoretical perspective, (Baudoin et al. (submitted a)) calculated analytically the orbital acoustic streaming produced by a Bessel spherical vortex. As the resolution of this problem from Eckart's equation is intricate, they proposed another method based on Equation 29 and the use of the Green function of Stokes equation. They showed that the resulting flow is a purely orbital (since φ is the only propagative component of a Bessel spherical vortex) with a confined flow structure located near the focal point.

SUMMARY POINTS

1. The manipulations of particles and fluids with acoustic waves are enabled by two nonlinear effects: acoustic radiation pressure and acoustic streaming respectively.
2. Since both acoustic and optical radiation pressure are proportional to the wave intensity divided by the sound speed, acoustical tweezers enable to apply forces several orders of magnitude larger than their optical counterpart at same wave intensity.
3. Acoustical tweezers relying on plane standing wave enable to trap and move particles collectively, but the multiplicity of nodes and antinodes does not enable to move one particle independently of other neighboring particles, i.e. to trap particles selectively.
4. To achieve selectivity, a localization of the acoustic energy is necessary. Since many particles of interest are trapped at the pressure nodes, focalized waves cannot be used in this case. Localized traps for this type of particles can be achieved with some specific wave structures called acoustical vortices, which enable to both focalize the

acoustic energy and obtain a pressure minimum at the focal point surrounded by a bright ring, that serves as a trap.
5. To achieve 3D selective trapping with a one-sided tweezers, it is necessary to generate a wave structure that enables to compensate the inclination of the particles to be pushed in the wave direction. This task can be be achieved with one sided focalized vortices.
6. Acoustical vortices can generate some localized flow structures, whose topology relies on the topology of the acoustical vortex.

FUTURE ISSUES

1. **Particles assembly**. The 3D selective manipulation of particles with acoustical tweezers has been recently demonstrated. It is essential in the future to demonstrate that is not only possible to capture particles individually but also to assemble them to form clusters of precisely assembled objects.
2. **Force calibration**. For applications, it would also be necessary to calibrate the force applied by the tweezers as a function of the input power. Indeed, this calibration of the force would lead (as in optics but with forces several orders or magnitude larger) to many applications, e.g. to study cells mechanotransduction or the resistance of bioobjects to mechanical solicitations.
3. **Further miniaturization**. A significant step has been recently achieved in the miniaturization of acoustical tweezers. Nevertheless, acoustic coherent sources exist up to GHz, paving the way toward micrometric and even submicrometric particles manipulation. The manipulation at this scale is both a technical and scientific challenge, since it is necessary to understand how acoustic radiation pressure and acoustic streaming will evolve at these scales.
4. **Harmless selective manipulation of biological objects**. It is also necessary to demonstrate that acoustical traps with large trapping force can be obtained at micrometric scales with harmless acoustic signals for biological objects. This is critical for all applications involving cells and microorganisms.
5. **Measurement of acoustic streaming induced by focalized acoustical vortices**. Quantitative comparisons between experimentally synthesized velocity fields and theoretical developments are still lacking.

DISCLOSURE STATEMENT

The authors are not aware of any affiliations, memberships, funding, or financial holdings that might be perceived as affecting the objectivity of this review.

ACKNOWLEDGMENTS

The authors would like to express their gratitude to the colleagues and students who, over the years, shared their views with us and made this review possible, in particular O. Bou Matar, D. Baresch, J.-C. Gerbedoen, R. Marchiano and A. Riaud.

LITERATURE CITED

Allen & Rudnick (1947). Allen CH, Rudnick I. 1947. A Powerful High Frequency Siren. *J. Acoust. Soc. Am.* 19:5,857–65

Altberg (1903). Altberg W. 1903. Ueber die Druckkräfte der Schallwellen und die absolute Messung der Schallintensitt *Ann. Physik* 316:6,405-420

Anhäuser, Wunenburger & Brasselet (2012). Anhäuser A, Wunenburger R, Brasselet E. 2012. Acoustical rotational manipulation using orbital angular momentum transfer *Phys. Rev. Lett.* 109:034301

Apfel (1981). Apfel RE. 1981. Acoustic levitation for studying liquids and biological materials. *J. Acoust. Soc. Am.* 70:2,636–39

Ashkin et al. (1986). Ashkin A, Dziedzic JM, Bjorkholm JE, Chu S. 1986. Observation of a single-beam gradient force optical trap for dielectric particles *Opt. Lett.* 11:5,288–290

Ashkin (2011). Ashkin A. 2011. How it all began *Nature Photon.* 5:6,316–317

Baird (1963). Baird MHI. 1963. Resonant Bubbles in a Vertically Vibrating Liquid Column. *Can. J. Chem. Eng.* 41:52–55

Baker (1972). Baker NV. 1972. Segregation and Sedimentation of Red Blood Cells in Ultrasonic Standing Waves *Nature* 239, 398–399

Baresch, Thomas & Marchiano (2013a). Baresch D, Thomas J-L, Marchiano, R. 2013. Three-dimensional acoustic radiation force on an arbitrarily located elastic sphere. *J. Acoust. Soc. Am.* 133:1,25–36

Baresch, Thomas & Marchiano (2013b). Baresch D, Thomas J-L, Marchiano, R. 2013. Spherical vortex beams of high radial degree for enhanced single-beam tweezers, *J. Appl. Phys.* 113:184901

Baresch (2014). Baresch D. 2014. Pince acoustique: piégeage et manipulation d'un objet par pression de radiation d'une onde progressive *Doctoral dissertation* https://tel.archives-ouvertes.fr/tel-01165034

Baresch, Thomas & Marchiano (2016). Baresch D, Thomas J-L, Marchiano, R. 2016. Observation of a single-beam gradient force acoustical trap for elastic particles: acoustical tweezers. *Phys. Rev. lett.* 116:024301

Baresch, Thomas & Marchiano (2018). Baresch D, Thomas J-L, Marchiano, R. 2018. Orbital angular momentum transfer to stably trapped elastic particles in acoustical vortex beams. *Phys. Rev. lett.* 121:074301

Barton, Alexander & Schaub (1988). Barton JP, Alexander DR, Schaub, SA. 1988. Internal and near-surface electromagnetic fields for a spherical particle irradiated by a focused laser beam. *J. Appl. Phys.* 4:1632–39

Barton, Alexander & Schaub (1989). Barton JP, Alexander DR, Schaub SA. 1989. Theoretical determination of net radiation force and torque for a spherical particle illuminated by a focused laser beam. *J. Appl. Phys.* 66:10,4594–4602

Baudoin et al. (2019a). Baudoin M, Gerbedoen J-C, Riaud A, Bou Matar O, Smagin N, Thomas J-L. 2019. Folding a focalized acoustical vortex on a flat holographic transducer: miniaturized selective acoustical tweezers. *Sci. Adv.* 5:eaav1967

Baudoin et al. (submitted a). Baudoin M, Kolumari R, Marchiano R, Thomas J-L. 2019. Orbital acoustic streaming induced by spherical vortex beams *Submitted*

Beissner (1998). Beissner K. 1998. The acoustic radiation force in lossless fluids in Eulerian and Lagrangian coordinates. *J. Acoust. Soc. Am.* 103:5,2321–32

Biquard (1932a). Biquard, P. 1932. Les ondes ultra-sonores. *Revue d'Acoustique* 1:93–109

Biquard (1932b). Biquard, P. 1932. Les ondes ultra-sonores II. *Revue d'Acoustique* 1:315–355

Bjerknes (1906). Bjerknes VFJ. 1906 . Fields of Force. *New York: Columbia University Press*

Bopp (1940). Bopp VF. 1940. Energetische Betrachtungen zum Schaallstrahlungsdruck *Ann. Physik* 38:5,495–500

Borgnis (1953). Borgnis FE. 1953. Acoustic Radiation Pressure of Plane compressional Waves. *Rev.*

Mod. Phys. 25:653–663

Brillouin 1925a. Brillouin L. 1925. Sur les tensions de radiation. *Ann. Phys. X* 4:528-586

Brillouin (1925b). Brillouin L. 1956. Les tensions de radiation ; leur interprétation en mécanique classique et en relativité. *Journal de Physique et le Radium* 6:11,337-353

Brillouin (1936). Brillouin L. 1936. Les pressions et tensions de radiation. *Revue d'Acoustique* 5:99–111

Brillouin (1938). Brillouin L. 1938. Tensors in mechanics and elasticity. *Academic Press, New York, 1964*

Bucchanan, Jameson & Oedjoe (1962). Buchanan RH, Jameson G, Oedjoe D. 1962. Cyclic migration of bubbles in vertically vibrating columns Ind. Eng. Chem. Fundamentals 1:2,82–86

Chen & Apfel (1996). Chen X, Apfel RE. 1996. Radiation force on a spherical object in the field of a focused cylindrical transducer. *J. Acoust. Soc. Am.* 101:5,2443–47

Coakley et al. (1989). Coakley WT, Bardsley DW, Grundy MA, Zamani F, Clarke DJ 1989. Cell Manipulation in Ultrasonic Standing Wave Fields *J. Chem. Tech. Biotechnol.* 44:43–62

Coulouvrat (1992). Coulouvrat F. 1992. On the equations of nonlinear acoustics *J. Acoust.* 5:321–359

Courtney (2014). Courtney CRP, Demore CEM, Wu H, Grinenko A, Wilcox PD, Cochran S, and Drinkwater BW. 2014. Independent trapping and manipulation of microparticles using dexterous acoustic tweezers *Appl. Phys. Lett.* 104: 154103

Ding et al. (2013). Ding X, Li P, Lin S-C, Stratton ZS, Nama N, Guo F, Slotcavage D, Mao X, Shi J, Costanzo F, Huang TJ 2013. Surface acoustic wave microfluidics *Lab Chip.* 13:18,362649

Ding et al. (2012). Ding X, Li P, Lin S-C, Kirali B, Yue H, Li X, Chiang I-K, Shi J, Benkovic SJ, Huang TJ 2013. On-chip manipulation of single microparticles, cells, and organisms using surface acoustic waves *P. Natl. Acad. Sci. USA* 109:28, 1110511109

Dvorak (1874). Dvorak V. 1874. Ueber die entstehunweise der Kundt'schen Staubfiguren. *Ann. Phys.* 227:4,634-639

Eckart (1948). Eckart C. 1948. Vortices and streams caused by sound waves. *Phys. Rev.* 73:1, 68-76

Einspruch, Witterholt & Truell (1960). Einspruch NG, Witterholt EJ, Truell R. 1960. Scattering of a plane transverse wave by a spherical obstacle in an elastic medium. *J. Appl. Phys.* 31:5,806-18

Eller (1968). Eller A. 1968. Force on a bubble in a standing acoustic wave. *J. Acoust. Soc. Am.* 43:1,170–171

Embleton (1954). Embleton TFW. 1954. Mean Force on a Sphere in a Spherical Sound Field. I. (Theoretical). *J. Acoust. Soc. Am.* 26:1,40–45

Faraday (1831). On a peculiar class of acoustical figures; an don certain forms assumed by groups of particles upon vibrating elastic surfaces *Phil. Trans. R. Soc. Lond.* 299:340

Faran (1951). Faran JJ. 1951. Sound scattering by solid cylinders and spheres. *J. Acoust. Soc. Am.* 23:405–418

Gaunard & Überall (1978). Gaunard GC, Überall H. 1978. Theory of resonant scattering from spherical cavities in elastic and viscoelastic media. *J. Acoust. Soc. Am.* 63:6,1699–712

Gorkov (1962). Gor'kov LP. 1962. On the forces acting on a small particle in an acoustic field in an ideal fluid. *Sov. Phys. Dokl* 6:773–75

Gouesbet, Lock & Gréhan (2010). Gouesbet G, Lock JA, Gréhan G. 2010 Generalized LorenzMie theories and description of electromagnetic arbitrary shaped beams : Localized approximations and localized beam models, a review. *J. Quant. Spect. and Rad. Transf.* 112:1–27

Gould (1968). Gould RK. 1968 Simple Method for Calibrating Small Omnidirectional Hydrophones *J. Acoust. Soc. Am.* 43:5,1185–87

Gusev & Rudenko (1979). Gusev VE, Rudenko OV. 1979. Nonsteady quasi-one-dimensional acoustic streaming in unbounded volumes with hydrodynamic nonlinearity *Sov. Phys. Acoust.* 25:6,493-497

Hagsäter et al. (2007). Hagsäter SM, Gladsam Jensen T, Bruus H, Kutter JP . 2007. Acoustic res-

onances in microfluidic chips: full-image micro-PIV experiments and numerical simulations. *Lab Chip* 7:1336–44

Hasegawa & Yosioka (1969). Hasegawa T, Yosioka K. 1969. Acoustic Radiation Force on a Solid Elastic Sphere. *J. Acoust. Soc. Am.* 46:5,1139–1143

Hasegawa (1977). Hasegawa T. 1977. Comparison of two solutions for acoustic radiation pressure on a sphere *J. Acoust. Soc. Am.* 61:6,1445–1448

Hasegawa, Ochi & Matsuzawa (1981). Hasegawa T, Ochi M, Matsuzawa K. Acoustic radiation force on a solid elastic sphere in a spherical wave field *J. Acoust. Soc. Am.* 69:4,937–942

Hasegawa et al. (2000). Hasegawa T, Kido T, Iizuka T, Matsuoka C. 2000. A general theory of Rayleigh and Langevin radiation pressures. *J. Acoust. Soc. Jpn.* 21:3,145–152

Hefner & Marston (1999). Hefner B.T., Marston P.L. 1999. An acoustical helicoidal wave transducer with applications for the alignment of ultrasonic and underwater systems *J. Acoust. Soc. Am.* 106:6,3313–16

Herrey (1955). Herrey EM. 1955. Experimental studies on acoustic radiation pressure. *J. Acoust. Soc. Am.* 27:891–896

Hertz & Mende (1939). Hertz G, Mende H. 1939. Der Schallstrahlungsdruk in Flussigkeiten. *Z. Physik* 114:354–367

Hong, Zhang & Drinkwater (2015). Hong Z, Zhang J, Drinkwater B. 2015. Observation of orbital angular momentum transfer from Bessel-shaped acoustic vortices to diphasic liquid-microparticle mixtures. *Phys. Rev. Lett* 114:21,214301

Jackson (1962). Jackson JD. 1962. Classical Electrodynamics. *John Wiley and Sons Inc.* Chap. 6

Jiang et al (2016). Jiang X., Li Y., Liang B., Cheng J-C., Zhang L. 2016. Convert Acoustic Resonances to Orbital Angular Momentum *Phys. Rev. Lett.* 117:034301

Jiménez et al (2016). Jiménez N., Picó R., Sánchez-Morcillo V., Romero-García V., García-Raffi L. M., Staliunas K. 2016 Formation of high-order acoustic Bessel beams by spiral diffraction gratings *Phys. Rev. E* 94:053004 (2016)

Kamakura (1996). Kamakura T, Sudo T, Matsuda K, Kumamoto Y. 1996. Time evolution of acoustic streaming from a planar ultrasound source. *J. Acoust. Soc. Am.* 100:1,132–138

Karlsen & Bruus (2015). Karlsen JT, Bruus H. 2015. Forces acting on a small particle in an acoustical field in a thermoviscous fluid *Phys. Rev. E* 92:043010

Karlsen & Bruus (2016). Karlsen JT, Augustsson P, Bruus H. 2016. Acoustic force density acting on inhomogeneous fluids in acoustic fields *Phys. Rev. Lett.* 117:114504

King (1934). King L. 1934. On the acoustic radiation pressure on spheres. *Proc. R. Soc. London A* 147:212–240

Klein (1938). Klein E. 1938. Absolute Sound Intensity in Liquids by Spherical Torsion Pendula *J. Acoust. Soc. Am.* 9:312–320

Kuznetsov (1970). Kuznetsov VP. 1970. Equations of nonlinear acoustics *Sov. Phys. Acoust.* 16:467–470

Lighthill (1978). Lighthill J. 1978. Acoustic streaming *J. Sound Vib.* 61(3):391–418

Lenshof & Laurell (2010). Lenshof A, Laurell T. 2010. Continuous separation of cells and particles in microfluidic systems *Chem. Soc. Rev.* 39:120317

Li et al (2015). Metascreen-Based Acoustic Passive Phased Array Li Y., Jiang X., Liang B., Cheng J-C., Zhang L. 2015. *Phys. Rev. Applied* 4:024003

Libermann (1949). Liberman, LN. 1949. The second viscosity of liquids. *Phys. Rev.* 75:1415–1422

Maheu, Gouesbet & Gréhan (1987). Maheu B, Gouesbet G, Gréhan, G. 1987. A concise presentation of the generalized Lorenz-Mie theory for arbitrary location of the scatterer in an arbitrary incident profile. *J. Opt.* 19:2, 59–67

Marston (2006). Marston, PL. 2006. Axial radiation force of a Bessel beam on a sphere and direction reversal of the force. *J. Acoust. Soc. Am.* 120:6,3518–

Marston (2008). Marston, PL. 2008. Scattering of a Bessel beam by a sphere: II helicoidal case and spherical shell example. *J. Acoust. Soc. Am.* 124:5,2905–10

Marston (2009). Marston, PL. 2009. Radiation force of a helicoidal Bessel beam on a sphere. *J. Acoust. Soc. Am.* 120:3539–47

Marston & Zhang (2017). Marston P. L., Zhang L. 2017. Relationship of scattering phase shifts to special radiation force conditions for spheres in axisymmetric wave-fields *J. Acoust. Soc. Am.* 141:5,3042–49

Marzo et al. (2015). Marzo A, Seah SA, Drinkwater BW, Sahoo DR, Long B, Subramanian S. 2015. Holographic acoustic elements for manipulation of levitated objects *Nature comm.* 6:8661

McIntyre (1981). McIntyre ME. 1981. On the "wave momentum" myth. *J. Fluid. Mech.* 106:331-347

Moudjed et al. (2014). Moudjed B, Botton V, Henry D, Ben Hadid H, Garandet J-P. 2014. Scaling and dimensional analysis of acoustic streaming jets. *Phys. Fluids* 26:093602

Neuman & Nagy (2008). Neuman KC, Nagy A. 2008. Single-molecule force spectroscopy: optical tweezers, magnetic tweezers and atomic force microscopy *Nature Meth.* 5:6,491–505

Nyborg (1953). Nyborg WL. 1953. Acoustic streaming due to attenuated plane waves *J. Acoust. Soc. Am.* 25:1,68–75

Nye & Berry (1974). Nye JF, Berry MV 1974. Dislocations in wave trains *Proc. Roy. Soc. London* 336:164–90

Ozcelik et al. (2018). Ozcelik A, Rufo J, Guo F, Gu Y, Li P, Lata J and Huang TJ 2018 Acoustic tweezers for the life sciences. *Nature Meth.* 15: 1021–1028

Peierls (1985). Peierls R. 1985. Momentum and pseudomomentum of light and sound. *Highlights of Condensed Matter Theory* 237-255

Post (1953). Post EJ. 1953. Radiation pressure and dispersion. *J. Acoust. Soc. Am.* 25:1,55–60

Post (1960). Post EJ. 1960. Meaning and interpretation of acoustic momentum and acoustic radiation. *Phys. Rev.* 118:5,1113–17

Rayleigh (1884). Lord Rayleigh. 1884. On the circulation of air observed in Kundt's tubes, and some allied acoustical problems, *Phil. Trans. R. Soc. Lond.* 175:1–21

Rayleigh (1902). Lord Rayleigh. 1902. On the pressure of vibration *Phil. Mag.* 3:338–346

Rayleigh (1905). Lord Rayleigh. 1905. On the momentum and pressure of gaseous vibrations, and on the connection with the virial theorem *Phil. Mag.* 10:364–374

Ren, Gréhan & Gouesbet (1994). Ren KF, Gréhan G, Gouesbet G. 1994. Radiation pressure forces exerted on a particle arbitrarily located in a gaussian beam by using the generalized Lorenz-Mie theory, and associated resonance effects. *Optics Comm.* 108:343–54

Riaud et al. (2014). Riaud A, Baudoin M, Thomas J-L, Bou Matar, O. 2014. Cyclones and attractive streaming generated by acoustical vortices. *Phys. Rev. E* 90:013008

Riaud et al. (2017a). Riaud A, Baudoin M, Bou Matar O, Becera L, Thomas J-L. 2017. Selective manipulation of microscopic particles with precursor swirling Rayleigh waves. *Phys. Rev. Appl.* 7:024007

Riaud et al. (2017b). Riaud A, Baudoin M, Bou Matar O, Thomas J-L, Brunet P. 2017. On the influence of viscosity and caustics on acoustic streaming in sessile droplets: an experimental and a numerical study with a cost-effective method. *J. Fluid. Mech.* 821:384–420

Richter (1940). Richter VG. 1940. Zur Frage des Schallstrahlungsdruckes. *G. Z. Physik* 115:97–108

Riley (2001). Riley N. 2001. Steady streaming. *Ann. Rev. Fluid Mech.* 33:43–65

Romanenko (1960). Riley N. 2001. Experimental study of acoustic streaming in water *Sov. Phys. Acoust.* 6:87–91

Rudenko (1971). Rudenko OV and Soluyan SI. 1971. Theory of non-stationary acoustic streaming *Sov. Phys. Acoust.* 17:97–101

Rooney (1973). Rooney JA. 1973. Determination of acoustic power outputs in the microwatt-milliwatt range *Ultrasound in Med. & Biol.* 1:13–16

Rudnick (1977). Rudnick I. 1977. Measurements of the acoustic radiation pressure on a sphere in a standing wave field. *J. Acoust. Soc. Am.* 62:5,20–22

Sapozhnikov & Bailey (2013). Sapozhnikov OA., Bailey MR. 2013. Radiation force of an arbitrary

acoustic beam on an elastic sphere in a fluid. *J. Acoust. Soc. Am.* 133:2,661–676

Schram (1984). Schram CJ. 1984. Separation of particles in liquid medium - using varied ultrasonic standing wave *European Patent* 167406

Settnes & Bruus (2012). Settnes M, Bruus H. 2012. Forces acting on a small particle in an acoustical field in a viscous fluid. *Phys. Rev. E* 85: 016327

Shiokawa (1990). Shiokawa S, Mastui Y, Ueda T. 1990. Study on SAW streaming and its application to fluid device. *Japan J. Appl. Phys.* 29 (Sup 29-1):137–139

Silva (2011). Silva, GT. 2011. An expression for the radiation force exerted by an acoustic beam with arbitrary wavefront. *J. Acoust. Soc. Am.* 130:6,3541–44

Sölner & Bondy (1936). Sölner K, Bondy C. 1936. The mechanism of coagulation by ultrasonic waves *Trans. Faraday Soc.* 32:616–623

Stanikov (1967). Stanikov YG. 1967. Streaming induced by finite amplitude sound *Sov. Phys. Acous.* 23:247–285

Svoboda & Block (1994). Svoboda K, Block SM. 1994. Biological applications of optical forces *Annu. rev. biophys. biomol. struct.* 23:247–285

Thomas, Marchiano & Baresch (2017). Thomas J-L, Marchiano R, Baresch D. 2017. Acoustical and optical radiation pressure and the development of single beam acoustical tweezers. *J. Quant. Spect. Rad. Transf.* 195:55–65

Tran, Marmottant & Thibault (2012). Tran, SBQ. Marmottant P, Thibault P. 2012. Fast acoustic tweezers for the two-dimensional manipulation of individual particles in microfluidic channels *Appl. Phys. Lett.* 101:114103

Whitworth, Grundy & Coakley (1991). Whitworth G, Grundy MA, Coakley WT 1991. Transport and harvesting particles using modulated ultrasound *Ultrasonics* 29:439–444

Xie & Wei (2002). Xie WJ, Wei B 2002. Dependence of acoustic levitation capabilities on geometric parameters *Phys. Rev. E* 66:026605

Yeo & Friend (2014). . Yeo LY, Friend JR 2014. Surface Acoustic Wave Microfluidics *Annu. Rev. Fluid Mech.* 46:379-406

Yosioka & Kawasima (1955). Yosioka K, Kawasima Y 1955. Acoustic radiation pressure on a compressible sphere. *Acustica* 5:3,167–173

Westervelt, P.J. (1953). Westervelt, PJ. 1953. The theory of steady rotational flow generated by a sound field *J. Acoust. Soc. Am.* 25:61,60–67

Wu (1991). Wu JR 1991 Acoustical tweezers *J. Acoust. Soc. Am.* 89:5,2140–2143